Nanosensors and spintronics

Jaroslav Hamrle

jaroslav.hamrle@vsb.cz

April 14, 2014

Outline

Quantum description of electron and its spin

Spin of particles (spin of electron):

- Consequence of relativity, but can be postulated as particle property.
- Electron (and also proton, neutron) has quantized spin $s = \frac{1}{2}$.

In following, we first postulate existence of spin. Then, we show how spin originates from relativistic quantum theory.

Angular momentum I

Total angular momentum = orbital angular momentum + spin angular momentum

Non-relativistic Schrödinger equation does not have spin (only angular momentum) ⇒ spin can be included *ad-hoc*.

Definition of angular momentum

$$\hat{\mathbf{L}} = \hat{\mathbf{r}} \times \hat{\mathbf{p}} = \frac{\hbar}{i} \hat{\mathbf{r}} \times \nabla \quad (1)$$

Commutation relations of angular momentum operator:

$$[\hat{L}_x, \hat{L}_y] = i\hbar \hat{L}_z \qquad [\hat{L}_y, \hat{L}_z] = i\hbar \hat{L}_x \quad (2)$$

$$[\hat{L}_z, \hat{L}_x] = i\hbar \hat{L}_y \qquad [\hat{\mathbf{L}}^2, \hat{L}_i] = 0 \quad (3)$$

and

$$[\hat{L}_x, \hat{y}] = -[\hat{L}_y, \hat{x}] = i\hbar \hat{z} \qquad [\hat{L}_x, \hat{p}_y] = -[\hat{L}_y, \hat{p}_x] = i\hbar \hat{p}_z \quad (4)$$

$$[\hat{L}_x, \hat{x}] = [\hat{L}_x, \hat{p}_x] = 0 \quad (5)$$

Example of determining commutators between angular momenta

E.g.

$$[L_x, L_y] = [(YP_z - ZP_y), (ZP_x - XP_Z)] = Y[P_z, Z]P_x + XP_Y[Z, P_Z]$$
$$= i\hbar(-YP_x + XP_y) = i\hbar L_z$$

Angular and spin momentum II

- Spin in non-relativistic description: intrinsic property of the electron

$\Rightarrow$ can not be defined similar to Eq. (1)

$\Rightarrow$ spin is defined as quantity obeying the same commutation equations as $\hat{\mathbf{L}}$.

- Total angular momentum

$$\hat{\mathbf{J}} = \hat{\mathbf{L}} + \hat{\mathbf{S}} \tag{6}$$

where $\hat{\mathbf{J}}$ obeys equal commutation relation.

Angular momentum III: eigenvalues

Total angular momentum eigenvalues:

$$\hat{\mathbf{J}}^2\psi_j^{m_j} = j(j+1)\hbar^2\psi_j^{m_j} \qquad (7)$$

$$\hat{J}_z\psi_j^{m_j} = m_j\hbar\psi_j^{m_j} \qquad (8)$$

where $-j \leq m_j \leq j$.

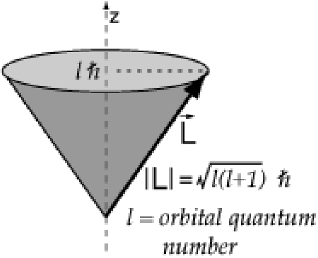

http://hyperphysics.phy-astr.gsu.edu/hbase/quantum/vecmod.html

Angular momentum IV: length of momentum

- Maximum value of J in z-direction is $|m_j| = j$
- However, length of J is $\sqrt{j(j+1)}$

$\Rightarrow$ angular momentum can never points exactly in z (or in any other) direction

- classical limit: $j \to \infty$

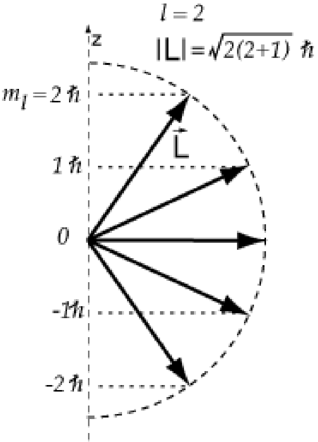

http://hyperphysics.phy-astr.gsu.edu/hbase/quantum/vecmod.html

Angular momentum V: raising/lowering operators

Lowering/raising operators:

$$\hat{J}_\pm = \hat{J}_x \pm i\hat{J}_y$$

- $J_+J_- = J_x^2 + J_y^2 + \hbar J_z = J^2 - J_z^2 + \hbar J_z$
- $J_-J_+ = J_x^2 + J_y^2 - \hbar J_z = J^2 - J_z^2 - \hbar J_z$
- $[J_z, J_+] = +\hbar J_+$
- $[J_z, J_-] = -\hbar J_-$
- $[J_+, J_-] = 2\hbar J_z$
- $[J^2, J_+] = [J^2, J_-] = [J^2, J_z] = 0$

Angular momentum V: raising/lowering operators

- value of m_j can be increased/decreased by raising/lowering operator $\hat{J}_\pm = \hat{J}_x \pm i\hat{J}_y$, working as

$$|\hat{J}_+|j,m_j\rangle = \hbar\sqrt{(j-m_j)(j+m_j+1)}\,|j,m_j+1\rangle$$

$$|\hat{J}_-|j,m_j\rangle = \hbar\sqrt{(j+m_j)(j-m_j+1)}\,|j,m_j-1\rangle$$

- Can be derived by two steps:
    - Apply $\hat{J}_\pm$ to eigenstate $|j,m_j\rangle$ (by using commutator relations; note: $|J_z|j,m_j\rangle = \hbar m_j\,|j,m_j\rangle$):

$$|\hat{J}_z\hat{J}_\pm|j,m_j\rangle = |\hat{J}_\pm\hat{J}_z + [\hat{J}_z,\hat{J}_\pm]|j,m_j\rangle = |\hat{J}_\pm\hat{J}_z + \hbar J_\pm|j,m_j\rangle =$$

$$(m_j\pm1)\hbar\,|\hat{J}_\pm|j,m_j\rangle = (m_j\pm1)\hbar\,|j,m_j\pm1\rangle = |\hat{J}_z|j,m_j\pm1\rangle$$

    - $|\,|J_+|j,m_j\rangle\,|^2 = \langle j,m_j|J_-J_+|j,m_j\rangle =$ $\langle j,m_j|J^2 - J_z^2 - \hbar J_z|j,m_j\rangle = \hbar^2[j(j+1) - m_j(m_j+1)]$ $\Rightarrow |J_+|j,m_j\rangle = \hbar\sqrt{j(j+1)-m_j(m_j+1)}\,|j,m_j\rangle =$ $\hbar\sqrt{(j-m_j)(j+m_j+1)}\,|j,m_j\rangle$

Angular momentum VI: particles with moment $s = 1/2$

The same valid for spin $j \to s = \frac{1}{2}$, $-s \leq m_s \leq s \Rightarrow m_s = 1/2$: spin-up spin ($\uparrow$); $m_s = -1/2$: spin-down spin ($\downarrow$)

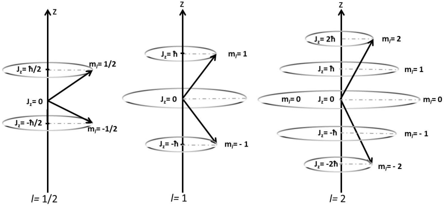

http://chemwiki.ucdavis.edu/Physical_Chemistry/Spectroscopy/

Non-relativistic Schrödinger equation

$$i\hbar\frac{\partial\psi_r(\vec{r},t)}{\partial t} = \frac{1}{2m}\left[\left(\frac{\hbar}{i}\nabla - e\vec{A}(\vec{r},t)\right)^2 + e\Phi(\vec{r},t)\right]\psi_r(\vec{r},t) \quad (9)$$

$$i\hbar\frac{\partial\psi_r(\vec{r},t)}{\partial t} = \hat{H}\psi_r(\vec{r},t) \quad (10)$$

where

- $A(\vec{r},t)$ is the vector potential ($\vec{B} = \nabla \times \vec{A}$)
- $e\Phi(\vec{r},t)$ is the scalar potential ($\vec{E} = -\nabla\Phi - \frac{\partial\vec{A}}{\partial t}$)

Schrödinger equation with spin

Spin can be superimposed into Schödinger equation by product of time-space dependent part $\psi_r(\vec{r},t)$ and spin-dependent part $\chi_s^{m_s}$

$$\psi_s^{m_s} = \psi_r(\vec{r},t)\chi_s^{m_s} \tag{11}$$

However, this is only valid when spin-freedom is strictly independent on its time-space part. This is not valid for e.g. spin-orbit coupling. Then, one can express spin-time-space wavefunction as

$$\psi(\vec{r},t) = c_\uparrow\psi_{r,\uparrow}(\vec{r},t)+c_\downarrow\psi_{r,\downarrow}(\vec{r},t) \equiv \begin{pmatrix} c_\uparrow\psi_{r,\uparrow}(\vec{r},t) \\ c_\downarrow\psi_{r,\downarrow}(\vec{r},t) \end{pmatrix} \approx \begin{pmatrix} c_\uparrow \\ c_\downarrow \end{pmatrix} \psi_r(\vec{r},t) \tag{12}$$

where following eigenvectors were used for definition

$$\chi_\uparrow = \begin{pmatrix} 1 \\ 0 \end{pmatrix} \qquad \chi_\downarrow = \begin{pmatrix} 0 \\ 1 \end{pmatrix} \tag{13}$$

Pauli matrices I

Now, we have spin-dependent part of the wavefunction $\chi_{\uparrow/\downarrow}$. The spin operators $\hat{\mathbf{S}}$ (equivalent of angular momentum operators $\hat{\mathbf{L}}$) are

$$\hat{S}_x = \frac{\hbar}{2}\tilde{\sigma}_x \qquad \hat{S}_y = \frac{\hbar}{2}\tilde{\sigma}_y \qquad \hat{S}_z = \frac{\hbar}{2}\tilde{\sigma}_z \tag{14}$$

where $\tilde{\sigma}_{x/y/z}$ are Pauli matrices

$$\tilde{\sigma}_x = \begin{pmatrix} 0 & 1 \\ 1 & 0 \end{pmatrix} \qquad \tilde{\sigma}_y = \begin{pmatrix} 0 & -i \\ i & 0 \end{pmatrix} \qquad \tilde{\sigma}_z = \begin{pmatrix} 1 & 0 \\ 0 & -1 \end{pmatrix} \tag{15}$$

Pauli matrices: mean values of S_x (output of measurements)

- Value of S_x for $\psi = |\uparrow\rangle = \begin{pmatrix} 1 \\ 0 \end{pmatrix}$:

$$\langle\psi|\hat{S}_x|\psi\rangle = \frac{\hbar}{2} \begin{pmatrix} 1 \\ 0 \end{pmatrix} \begin{pmatrix} 0 & 1 \\ 1 & 0 \end{pmatrix} \begin{pmatrix} 1 \\ 0 \end{pmatrix} = 0 \qquad (16)$$

- Value of S_x for $\psi = \frac{1}{\sqrt{2}} \begin{pmatrix} 1 \\ 1 \end{pmatrix}$:

$$\langle\psi|\hat{S}_x|\psi\rangle = \frac{\hbar}{2} \frac{1}{\sqrt{2}} \frac{1}{\sqrt{2}} \begin{pmatrix} 1 \\ 1 \end{pmatrix} \begin{pmatrix} 0 & 1 \\ 1 & 0 \end{pmatrix} \begin{pmatrix} 1 \\ 1 \end{pmatrix} = \frac{\hbar}{2} \qquad (17)$$

- Value of S_x for $\psi = \frac{1}{\sqrt{2}} \begin{pmatrix} 1 \\ i \end{pmatrix}$:

$$\langle\psi|\hat{S}_x|\psi\rangle = \frac{\hbar}{2} \frac{1}{\sqrt{2}} \frac{1}{\sqrt{2}} \begin{pmatrix} 1 \\ -i \end{pmatrix} \begin{pmatrix} 0 & 1 \\ 1 & 0 \end{pmatrix} \begin{pmatrix} 1 \\ i \end{pmatrix} = 0 \qquad (18)$$

Pauli matrices II

Properties of Pauli matrices

- $\tilde{\sigma}_k^2 = \mathbf{1}, \qquad \text{where} \quad k = \{x, y, z\}$
- $\tilde{\sigma}_x \tilde{\sigma}_y + \tilde{\sigma}_y \tilde{\sigma}_x = 0$ etc. for others subscripts
- $\tilde{\sigma}_x \tilde{\sigma}_y - \tilde{\sigma}_y \tilde{\sigma}_x = -2i\tilde{\sigma}_z$ etc. for others subscripts
- raising operator: $\hat{S}_+ = \hat{S}_x + i\hat{S}_y = \hbar \begin{pmatrix} 0 & 1 \\ 0 & 0 \end{pmatrix}$
- lowering operator: $\hat{S}_- = \hat{S}_x - i\hat{S}_y = \hbar \begin{pmatrix} 0 & 0 \\ 1 & 0 \end{pmatrix}$

Pauli matrices III: eigenvalues and eigenvectors

Properties of Pauli matrices

- eigenvector and eigenvalues of $\hat{S}_z$:
  - $\hat{S}_z\chi_\uparrow = \frac{\hbar}{2}\begin{pmatrix}1 & 0\\ 0 & -1\end{pmatrix}\begin{pmatrix}1\\ 0\end{pmatrix} = \frac{\hbar}{2}\chi_\uparrow$
  - $\hat{S}_z\chi_\downarrow = \frac{\hbar}{2}\begin{pmatrix}1 & 0\\ 0 & -1\end{pmatrix}\begin{pmatrix}0\\ 1\end{pmatrix} = -\frac{\hbar}{2}\chi_\downarrow$
  - in another words $\langle\chi_{\uparrow/\downarrow}|\hat{\mathbf{S}}_z|\chi_{\uparrow/\downarrow}\rangle = \hbar\,\langle\chi_{\uparrow/\downarrow}|m_\pm|\chi_{\uparrow/\downarrow}\rangle = \hbar m_\pm = \pm\hbar/2$
- eigenvector and eigenvalue of $\hat{\mathbf{S}}^2$:
  - $\hat{\mathbf{S}}^2\chi_{\uparrow/\downarrow} = (\hat{S}_x^2 + \hat{S}_y^2 + \hat{S}_z^2)\chi_{\uparrow/\downarrow} = \frac{3}{4}\hbar^2\begin{pmatrix}1 & 0\\ 0 & 1\end{pmatrix}\chi_{\uparrow/\downarrow} = \frac{3}{4}\hbar^2\chi_{\uparrow/\downarrow} = s(s+1)\hbar^2\chi_{\uparrow/\downarrow}$, where $s = 1/2$.
  - in another words: $\langle\chi_{\uparrow/\downarrow}|\hat{\mathbf{S}}^2|\chi_{\uparrow/\downarrow}\rangle = \hbar^2\,\langle\chi_{\uparrow/\downarrow}|s(s+1)|\chi_{\uparrow/\downarrow}\rangle = \hbar^2 s(s+1) = \frac{3\hbar^2}{4}$

Pauli matrices IV: derivation of $\hat{S}_x$, $\hat{S}_y$

- $\hat{J}_\pm = \hat{J}_x \pm i\hat{J}_y$
  $\Rightarrow \hat{J}_x = (\hat{J}_+ + \hat{J}_-)/2,\ \hat{J}_y = (\hat{J}_+ - \hat{J}_-)/(2i)$
- $\hat{J}_x \left|\chi_j^m\right\rangle = (\hat{J}_+ + \hat{J}_-) \left|\chi_j^m\right\rangle =$
  $\frac{1}{2}\hbar\sqrt{j(j+1) - m(m+1)} \left|\chi_j^{m+1}\right\rangle +$
  $\frac{1}{2}\hbar\sqrt{j(j+1) - m(m-1)} \left|\chi_j^{m-1}\right\rangle$
- using this equation, the $\hat{S}_x = \frac{\hbar}{2}\tilde{\sigma}_x$ can be constructed

	1/2,1/2>	**1/2,-1/2>**
<1/2,1/2	**0**	**1/2**
<1/2,-1/2	**1/2**	**0**

= <lx>

and hence Pauli matrix $\tilde{\sigma}_x$ derived.

Addition of angular momentum I

Let us assume two angular momenta $\vec{L}$ and $\vec{S}$ (but can be also $\vec{J}_1$ and $\vec{J}_2$). Then, we ask about eigenvector and eigenvalues of summation

$$\hat{\mathbf{J}} = \hat{\mathbf{L}} + \hat{\mathbf{S}} \tag{19}$$

Commutation relations:

$$[\hat{\mathbf{J}}^2, \hat{\mathbf{L}}^2] = [\hat{\mathbf{J}}^2, \hat{\mathbf{S}}^2] = 0 \tag{20}$$

$$[\hat{J}_z, \hat{\mathbf{L}}^2] = [\hat{J}_z, \hat{\mathbf{S}}^2] = 0 \tag{21}$$

$$[\hat{S}_z, \hat{J}_z] = [\hat{L}_z, \hat{J}_z] = 0 \tag{22}$$

$$\hat{\mathbf{J}}^2 = \hat{\mathbf{L}}^2 + \hat{\mathbf{S}}^2 + 2\hat{\mathbf{L}} \cdot \hat{\mathbf{S}} = \tag{23}$$

$$= \hat{\mathbf{L}}^2 + \hat{\mathbf{S}}^2 + 2\hat{L}_z\hat{S}_z + \hat{L}_+\hat{S}_- + \hat{L}_-\hat{S}_+ \tag{24}$$

Addition of angular momentum II

- Proper vector (from bases of proper vector of $\vec{L}$ and $\vec{S}$):

$$|l, l_z\rangle \oplus |s, s_z\rangle = |l, s, l_z, s_z\rangle \tag{25}$$

  being eigenstates for operators $\hat{\mathbf{L}}^2$, $\hat{\mathbf{S}}^2$, $\hat{L}_z$, $\hat{S}_z$ (with eigenvalues ...$l(l+1)\hbar^2$ etc.); $\oplus$ being tonsorial multiplication.
- However, commutation relations also show, that operators $\hat{\mathbf{J}}^2$, $\hat{\mathbf{J}}_z$, $\hat{\mathbf{L}}^2$, $\hat{\mathbf{S}}^2$ commute with operators $\hat{\mathbf{L}}^2$, $\hat{\mathbf{S}}^2$, $\hat{L}_z$, $\hat{S}_z$ $\Rightarrow$ there must be possibility to write previous eigenvectors in a new base of eigenvectors, being eigenstates of $\hat{\mathbf{J}}^2$, $\hat{\mathbf{J}}_z$, $\hat{\mathbf{L}}^2$, $\hat{\mathbf{S}}^2$ operators, being $|J, M\rangle$.

Addition of angular momentum III: Clebsch-Gordon coefficients

- So we have two bases of eigenvectors, describing the same wavefunctions ⇒ linear relation between them must exist

$$|J, M\rangle = \sum_{s_z=-s}^{s} \sum_{l_z=-l}^{l} |l, s, l_z, s_z\rangle \langle l, s, l_z, s_z|J, M\rangle \tag{26}$$

  where $\langle l, s, l_z, s_z|J, M\rangle$ are called Clebsch-Gordon coefficients. (Note: $|J, M\rangle$ should be named $|J, M, l, s\rangle$).
- Clebsch-Gordon coefficients $\langle l, s, l_z, s_z|J, M\rangle$ are non-zero when

$$M = l_z + s_z \tag{27}$$

$$|l - s| \leq J \leq l + s \tag{28}$$

Clebsch-Gordon coefficients: example I

$l = 1/2$, $s = 1/2$: **two spins**

- $M = 1$, $J = 1$

	$J=1$
$\|\uparrow,\uparrow\rangle$	1

- $M = 0$, $J = \{1, 0\}$

	$J=1$	$J=0$
$\|\uparrow,\downarrow\rangle$	$\sqrt{1/2}$	$\sqrt{1/2}$
$\|\downarrow,\uparrow\rangle$	$\sqrt{1/2}$	$-\sqrt{1/2}$

- $M = -1$, $J = 1$

	$J=1$
$\|\downarrow,\downarrow\rangle$	1

Clebsch-Gordon coefficients: example II

$l = 1$, $s = 1/2$: **spin + orbital angular momentum** $l = 1$

- $M = 3/2$, $J = 3/2$

	$J = 3/2$
$\|l_z = 1, \uparrow\rangle$	1

- $M = 1/2$, $J = \{3/2, 1/2\}$

	$J = 3/2$	$J = 1/2$
$\|l_z = 1, \downarrow\rangle$	$\sqrt{1/3}$	$\sqrt{2/3}$
$\|l_z = 0, \uparrow\rangle$	$\sqrt{2/3}$	$-\sqrt{1/3}$

- $M = -3/2$, $J = 3/2$

	$J = 3/2$
$\|l_z = -1, \downarrow\rangle$	1

Other symmetric coefficients writes:

$$\langle j_1 j_2; m_1 m_2 | j_1 j_2; jm\rangle = (-1)^{j-j_1-j_2} \langle j_1 j_2; -m_1, -m_2 | j_1 j_2; j, -m\rangle$$

$$\langle j_1 j_2; m_1 m_2 | j_1 j_2; jm\rangle = (-1)^{j-j_1-j_2} \langle j_2 j_1; m_2 m_1 | j_1 j_2; jm\rangle$$

Clebsch-Gordon coefficients: example III

$l = 2$, $s = \frac{1}{2}$: spin + orbital angular momentum $l = 2$

- $M = \frac{5}{2}$, $J = \frac{5}{2}$

	$J = \frac{5}{2}$
$\lvert l_z = 2, \uparrow\rangle$	1

- $M = \frac{3}{2}$, $J = \{\frac{5}{2}, \frac{3}{2}\}$

	$J = \frac{5}{2}$	$J = \frac{3}{2}$
$\lvert l_z = 2, \downarrow\rangle$	$\sqrt{\frac{1}{5}}$	$\sqrt{\frac{4}{5}}$
$\lvert l_z = 1, \uparrow\rangle$	$\sqrt{\frac{4}{5}}$	$-\sqrt{\frac{1}{5}}$

- $M = \frac{1}{2}$, $J = \{\frac{5}{2}, \frac{3}{2}\}$

	$J = \frac{5}{2}$	$J = \frac{3}{2}$
$\lvert l_z = 1, \downarrow\rangle$	$\sqrt{\frac{2}{5}}$	$\sqrt{\frac{3}{5}}$
$\lvert l_z = 0, \uparrow\rangle$	$\sqrt{\frac{3}{5}}$	$-\sqrt{\frac{2}{5}}$

- and $M = -\frac{1}{2}$, $M = -\frac{3}{2}$, $M = -\frac{5}{2}$ to be added accordingly

Zeeman effect

Splitting of energy levels by (external) magnetic field, due to Hamiltonian term $H_{\text{Zeeman}} = -\vec{\mu}_B \cdot \vec{B}$

1. splitting due to magnetic moment related with orbital angular momentum; odd number of lines, $l(l+1)$

$$\vec{\mu}_L = -\frac{\mu_B}{\hbar}\vec{L} = -g_L\frac{\mu_B}{\hbar}\vec{L} \tag{29}$$

   where $\mu_B = \frac{e\hbar}{2m_e}$ is Bohr magneton

2. splitting due to presence of spin of the electron (non-quantized electromagnetic field), atomic number Z is odd, even number of lines, $\uparrow, \downarrow$

$$\vec{\mu}_S = -2\frac{\mu_B}{\hbar}\vec{S} = -g_e\frac{\mu_B}{\hbar}\vec{S} \tag{30}$$

   (with quantized electromagnetic field, $2 \rightarrow 2.0023 = g_e$ for electron, so-called g-factor)

Zeeman effect in weak magnetic field I

Magnetic moment of total angular momentum is

$$\vec{\mu}_J = -g_J \frac{\mu_B}{\hbar} \vec{J} = -\frac{\mu_B}{\hbar}(g_L \vec{L} + g_S \vec{S}) \tag{31}$$

Hamiltonian's form assumes:

1. J commutes with remaining Hamiltonian terms (follows from central symmetry of atomic potential in case of atoms)
2. H_{Zeeman} is small and hence perturbation theory can be used (i.e. solution found in eigenstates of unperturbated Hamiltonian)

Then:

$$H_{\mathrm{Zeeman}} = -\vec{\mu}_J \cdot \vec{B} = g_J \omega_{\mathrm{Larmor}} J_z = \omega_{\mathrm{Larmor}}(L_z + 2S_z) \tag{32}$$

where $\omega_{\mathrm{Larmor}} = -\frac{\mu_B}{\hbar} B$ is the Larmor frequency

Zeeman effect in weak magnetic field II

Eigen-energy is found to be

$$E_{\text{Zeeman}} = g_J M \hbar \omega_{\text{Larmor}} \tag{33}$$

M being magnetic number and g-factor being

$$g_J = \frac{3}{2} + \frac{S(S+1) - L(L+1)}{2J(J+1)} \tag{34}$$

splitting into $2J+1$ levels.

Zeeman effect: weak magnetic field

$E_{\text{Zeeman}} = g_J M \hbar \omega_{\text{Larmor}}$
$\Rightarrow$ Splitting according total magnetic number M;
$-J \leq M \leq J$

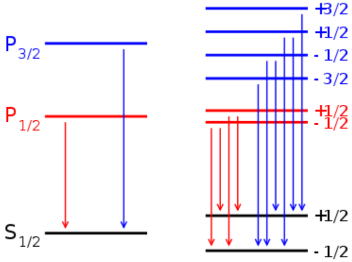

Zeeman effect: strong magnetic field

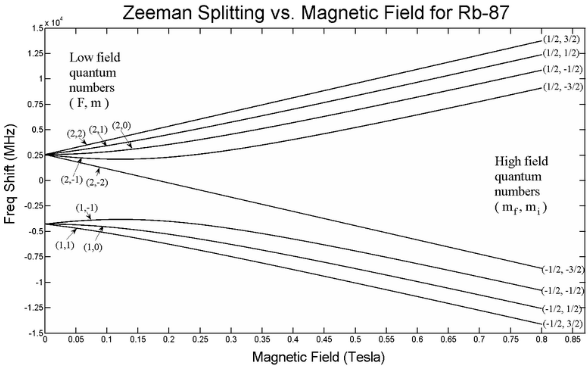

In this example of Rubidium (^{87}Rb):

without field: splitting by total angular momentum F, where $\vec{F} = \vec{J} + \vec{I}$; I is nucleus momentum

weak field: splitting of F-levels by their magnetic numbers m_F

large field: splitting by magnetic numbers m_F, m_I

http://en.wikipedia.org/wiki/Zeeman_effect

Special relativity I

Postulates of special relativity:

1. No preferential coordinate system exists; there is no absolute speed of translation motion.
2. Speed of light is constant in vacuum, for any observer or any source motion.

Let's assume to have two coordinate systems (x, y, z, ict) and (x', y', z', ict')

1. moving by mutual speed v along x and x' axis
2. in time $t = t' = 0$, both system intersects, $x = x'$, $y = y'$, $z = z'$
3. in time $t = t' = 0$, light pulse is generated

Special relativity II: Lorentz transformation

Then:

- $y = y'$, $z = z'$ as movement only along x, x'
- for $x' = 0$, $x = vt$
- for $x = 0$, $x' = -vt'$
- both systems see light pulse as a ball propagating by speed of light having diameter ct, ct' $\Rightarrow$
  $x^2 + y^2 + z^2 - c^2t^2 = x'^2 + y'^2 + z'^2 - c^2t'^2 \Rightarrow$
  $x^2 - c^2t^2 = x'^2 - c^2t'^2$.

Solutions of those equations:

$$x' = \frac{x - vt}{\sqrt{1 - \frac{v^2}{c^2}}} \qquad x = \frac{x' + vt'}{\sqrt{1 - \frac{v^2}{c^2}}} \tag{35}$$

$$t' = \frac{t - x\frac{v}{c^2}}{\sqrt{1 - \frac{v^2}{c^2}}} \qquad t = \frac{t' + x'\frac{v}{c^2}}{\sqrt{1 - \frac{v^2}{c^2}}} \tag{36}$$

Special relativity III: Lorentz transformation as matrix

This can be written in form of 4-vector (for space-time coordinate) and Lorenz transformation is 4×4 matrix:

$$\begin{bmatrix} x' \\ y' \\ z' \\ ict' \end{bmatrix} = \begin{bmatrix} \frac{1}{\sqrt{1-\frac{v^2}{c^2}}} & 0 & 0 & \frac{i\frac{v}{c}}{\sqrt{1-\frac{v^2}{c^2}}} \\ 0 & 1 & 0 & 0 \\ 0 & 0 & 1 & 0 \\ -\frac{i\frac{v}{c}}{\sqrt{1-\frac{v^2}{c^2}}} & 0 & 0 & \frac{1}{\sqrt{1-\frac{v^2}{c^2}}} \end{bmatrix} \begin{bmatrix} x \\ y \\ z \\ ict \end{bmatrix} \tag{37}$$

Special relativity IV: 4-vectors and invariants I

Let us define a general 4-vector $A_\mu = [A_1, A_2, A_3, A_4]$, which transform under equal Lorentz transformation, $A'_\mu = a_{\mu\nu} A_\nu$. Then, it can be shown that scalar multiplication of two four-vectors, $A_\mu B_\mu$ is invariant, i.e. the same in all cartesian systems related by Lorentz transformations.

→ **4-vector of space-time:** $x_\mu = [x, y, z, ict]$.

Space-time invariant: $x_\mu x_\mu = s^2 = x^2 + y^2 + z^2 - c^2 t^2$

proper time $\mathrm{d}\tau$ (or proper time interval)

$$\mathrm{d}\tau = \mathrm{d}t \sqrt{1 - \frac{V^2}{c^2}} = \mathrm{d}t' \sqrt{1 - \frac{V'^2}{c^2}} \qquad (38)$$

where V, V' is speed of the particle in both coordinate systems.

Special relativity IV: 4-vectors and invariants II

→ **4-vector of speed:**

$$U_\mu = \frac{\mathrm{d}x_\mu}{\mathrm{d}\tau} = \frac{1}{\sqrt{1-\frac{v^2}{c^2}}}\begin{bmatrix} v_x \\ v_y \\ v_z \\ ic \end{bmatrix} \tag{39}$$

Speed invariant: $U_\mu U_\mu = -c^2$

Special relativity V: 4-vectors of linear momentum

→ **4-vector of linear momentum:**

$$P_\mu = m_0 U_\mu \tag{40}$$

Then, linear momentum has form

$$P_\mu = \begin{bmatrix} \frac{m_0 v_x}{\sqrt{1-\frac{v^2}{c^2}}} \\ \frac{m_0 v_y}{\sqrt{1-\frac{v^2}{c^2}}} \\ \frac{m_0 v_z}{\sqrt{1-\frac{v^2}{c^2}}} \\ \frac{iW}{c} \end{bmatrix} \tag{41}$$

where $W = \frac{m_0 c^2}{\sqrt{1-\frac{v^2}{c^2}}} = m_0 c^2 + \frac{1}{2} m_0 v^2 + \cdots$ is a total particle energy.

Special relativity V: 4-vectors of linear momentum

- Linear momentum and energy of the particle are not independent, but as two pictures of the same quantity, as they are expressed by a components of single 4-vector
- Linear momentum invariant: $P_\mu P_\mu = -m_0^2 c^2 = \vec{p}^2 - W^2/c^2$
- Another expression of the total energy W:

$$W^2 = \vec{p}^2 c^2 + (m_0 c^2)^2 \tag{42}$$

being base of Dirac equation derived later.

Maxwell equations: 4-vector of current I

Conservation of charge: $\nabla \cdot \vec{J} + \frac{\mathrm{d}\rho}{\mathrm{d}t} = 0$
Rewritten into four-vector:

$$J_\mu = \begin{bmatrix} J_x \\ J_y \\ J_z \\ ic\rho \end{bmatrix} = \rho_0 U_\mu \tag{43}$$

where ρ_0 is charge density in rest system and then

$$\square \cdot J_\mu = 0 \tag{44}$$

where $\square$ is generalized Nabla operator,

$$\square = \left[\frac{\mathrm{d}}{\mathrm{d}x}, \frac{\mathrm{d}}{\mathrm{d}y}, \frac{\mathrm{d}}{\mathrm{d}z}, \frac{\mathrm{d}}{\mathrm{d}(ict)} \right]^T \tag{45}$$

Maxwell equations: 4-vector of current II

Then transformation of the current 4-vector leads to (speed v along x-axis)

$$J'_x = \frac{J_x - v\rho}{\sqrt{1-\frac{v^2}{c^2}}} \qquad J'_y = J_y \tag{46}$$

$$\rho' = \frac{\rho - \frac{v}{c^2}J_x}{\sqrt{1-\frac{v^2}{c^2}}} \qquad J'_z = J_z \tag{47}$$

- for example, charge is increasing with increasing v
- for small speeds ($v \ll c$), $J'_x = J_x - v\rho$

Maxwell equations: 4-vector of potential I

Maxwell equations expressed by potentials $\vec{A}$ and Φ

$$\nabla^2 \vec{A} - \frac{1}{c^2}\frac{\partial^2 \vec{A}}{\partial^2 t} = -\mu \vec{J} \tag{48}$$

$$\nabla^2 \Phi - \frac{1}{c^2}\frac{\partial^2 \Phi}{\partial^2 t} = -\frac{\rho}{\epsilon} \tag{49}$$

$$\nabla \cdot \vec{A} + \frac{1}{c^2}\frac{\partial \Phi}{\partial t} = 0 \tag{50}$$

where $\vec{B} = \nabla \times \vec{A}$ and $\vec{E} = -\nabla\Phi - \frac{\partial \vec{A}}{\partial t}$

Maxwell equations: 4-vector of potential II

The potential-written Maxwell equations as 4-vector simply writes

$$\Box^2 A_\mu = -\mu J_\mu \tag{51}$$

where 4-vectors A_μ, J_μ are

$$A_\mu = \begin{bmatrix} A_x \\ A_y \\ A_z \\ \frac{i\Phi}{c} \end{bmatrix} \qquad J_\mu = \begin{bmatrix} J_x \\ J_y \\ J_z \\ ic\rho \end{bmatrix} \tag{52}$$

Maxwell equations and special relativity I

Relation between 4-vector potential A_μ and E, B field expressed by antisymmetric tensor $f_{\mu\nu}$

$$f_{\mu\nu} = \frac{\partial A_\nu}{\partial x_\mu} - \frac{\partial A_\mu}{\partial x_\nu} = \begin{bmatrix} 0 & B_z & -B_y & -\frac{iE_x}{c} \\ -B_z & 0 & B_x & -\frac{iE_y}{c} \\ B_y & -B_x & 0 & -\frac{iE_z}{c} \\ \frac{iE_x}{c} & \frac{iE_y}{c} & \frac{iE_z}{c} & 0 \end{bmatrix} \tag{53}$$

Then, using electromagnetic tensor $f_{\mu\nu}$, Maxwell equations are

$$\frac{\partial f_{\lambda\rho}}{\partial x_\nu} + \frac{\partial f_{\rho\nu}}{\partial x_\lambda} + \frac{\partial f_{\nu\lambda}}{\partial x_\rho} = 0 \qquad (\nabla \times \vec{E} = -\partial \vec{B}/\partial t, \quad \nabla \cdot \vec{B} = 0) \tag{54}$$

$$\sum_\nu \frac{\partial f_{\mu\nu}}{\partial x_\nu} = \mu_0 J_\mu \qquad (\nabla \times \vec{B} = \mu_0 \vec{J} + c^{-2} \partial \vec{E}/\partial t, \quad \nabla \cdot \vec{E} = \rho/\epsilon) \tag{55}$$

Maxwell equations and special relativity II

The Lorentz transformation for electromagnetic field are

$$\vec{E}'_{\parallel} = \vec{E}_{\parallel} \qquad \vec{B}'_{\parallel} = \vec{B}_{\parallel} \tag{56}$$

$$\vec{E}'_{\perp} = \frac{(\vec{E} + \vec{v} \times \vec{B})_{\perp}}{\sqrt{1 - \frac{v^2}{c^2}}} \qquad \vec{B}'_{\perp} = \frac{(\vec{B} - \vec{v}/c^2 \times \vec{E})_{\perp}}{\sqrt{1 - \frac{v^2}{c^2}}} \tag{57}$$

i.e. for small speeds, $\vec{E}' = \vec{E} + \vec{v} \times \vec{B}$ and $\vec{B}' = \vec{B}$

Dirac equation: introduction I

Lorentz transformation unites time and space ⇒ relativistic quantum theory must do the same. Schrodinger equation does not fulfils this, as it it has first derivative in time and second in space.

1. Let as ASSUME, the Dirac equation will have first derivative in time. Then, it must be also in first derivative in space.
2. We want linear equations, for the principle of superposition.

Dirac equation: introduction II

Relativistic theory expresses total energy of the particle as:

$$W^2 = p^2c^2 + m_0^2c^4 \tag{58}$$

Quantum operator substitution: $\vec{p} \to \hat{\mathbf{p}} = -i\hbar\nabla$,
$W \to \hat{W} = i\hbar\partial/\partial t$. It follows in Klein-Gordon equation

$$\left(\nabla^2 - \frac{1}{c^2}\frac{\partial^2}{\partial t^2} - \frac{m_0^2c^2}{\hbar^2}\right)\psi(\vec{r},t) = 0 \tag{59}$$

This Eq. reduces to Eq. (58) for plane wave (free particle) $\psi(\vec{r},t) = \exp[i(\vec{r}\cdot\vec{p} - Wt)/\hbar]$. This condition limits following solutions to particles with spin $1/2$, as space-time wavefunction is symmetric, and hence spin-part must be antisymmetric.

Dirac equation: derivation I

As told above, let us assumed for Dirac equation:

1. linear in time and space derivatives
2. must fulfil Klein-Gordon equation, Eq. (59)
3. wave function is superposition of N base wavefunctions $\psi(\vec{r},t) = \sum \psi_n(\vec{r},t)$

General expression of condition 1:

$$\frac{1}{c}\frac{\partial \psi_i(\vec{r},t)}{\partial t} = -\sum_{k=x,y,z}\sum_{n=1}^{N} \alpha_{i,n}^{k} \frac{\partial \psi_n}{\partial k} - \frac{imc}{\hbar}\sum_{n=1}^{N} \beta_{i,n}\psi_n(\vec{r},t) \quad (60)$$

Dirac equation: derivation II

When expressed in matrix form (ψ is column vector, $\alpha^k_{i,n}$ is $3 \times N \times N$ matrix, $\beta_{i,n}$ is $N \times N$ matrix)

$$\frac{1}{c}\frac{\partial\psi(\vec{r},t)}{\partial t} = -\tilde{\boldsymbol{\alpha}} \cdot \nabla\psi(\vec{r},t) - \frac{imc}{\hbar}\tilde{\beta}\psi(\vec{r},t) \tag{61}$$

Substituting quantum operators $\hat{\mathbf{p}} \to \hbar\nabla/i$, we get Dirac equation

$$i\hbar\frac{\partial\psi(\vec{r},t)}{\partial t} = \hat{H}\psi(\vec{r},t) = (c\tilde{\boldsymbol{\alpha}} \cdot \hat{\mathbf{p}} + \tilde{\beta}mc^2)\psi(\vec{r},t) \tag{62}$$

where matrices $\tilde{\alpha}$, $\tilde{\beta}$ are unknown.

Dirac equation: properties I

Comparing total energy of the particle between relativity and Dirac Hamiltonian

$$W = \sqrt{p^2c^2 + m^2c^4} = \boldsymbol{\alpha} \cdot \vec{p}c + \beta mc^2 \tag{63}$$

Calculating W^2, we obtain conditions on α and β

$$\alpha_x^2 = \alpha_y^2 = \alpha_z^2 = \beta^2 = 1 \tag{64}$$

$$\alpha\beta + \beta\alpha = 0 \tag{65}$$

$$\alpha_x\alpha_y + \alpha_y\alpha_x = \alpha_y\alpha_z + \alpha_z\alpha_y = \alpha_z\alpha_x + \alpha_x\alpha_z = 0 \tag{66}$$

No numbers can fulfils those conditions for α and β; but α, β can be matrices.

Dirac equation: properties II

$$\alpha_x^2 + \alpha_y^2 + \alpha_z^2 = \beta^2 = 1 \qquad (67)$$

$$\alpha\beta + \beta\alpha = 0 \qquad (68)$$

$$\alpha_x\alpha_y + \alpha_y\alpha_x = \alpha_y\alpha_z + \alpha_z\alpha_y = \alpha_z\alpha_x + \alpha_x\alpha_z = 0 \qquad (69)$$

- We need four matrices, with (i) square is identity and (ii) which anti-commute each other.
- Three 2×2 Pauli matrices anticommute each other, but they are only three.

$\Rightarrow$ one must use matrices 4×4.

$\rightarrow$ several sets of those 4×4 can be found.

Dirac equation: Dirac matrices

One of the form of Dirac matrices α and β is

$$\tilde{\alpha}_x = \begin{bmatrix} 0 & 0 & 0 & 1 \\ 0 & 0 & 1 & 0 \\ 0 & 1 & 0 & 0 \\ 1 & 0 & 0 & 0 \end{bmatrix} = \begin{bmatrix} 0 & \tilde{\sigma}_x \\ \tilde{\sigma}_x & 0 \end{bmatrix} \qquad \tilde{\alpha}_y = \begin{bmatrix} 0 & 0 & 0 & -i \\ 0 & 0 & i & 0 \\ 0 & -i & 0 & 0 \\ i & 0 & 0 & 0 \end{bmatrix} = \begin{bmatrix} 0 & \tilde{\sigma}_y \\ \tilde{\sigma}_y & 0 \end{bmatrix} \tag{70}$$

$$\tilde{\alpha}_z = \begin{bmatrix} 0 & 0 & 1 & 0 \\ 0 & 0 & 0 & -1 \\ 1 & 0 & 0 & 0 \\ 0 & -1 & 0 & 0 \end{bmatrix} = \begin{bmatrix} 0 & \tilde{\sigma}_z \\ \tilde{\sigma}_z & 0 \end{bmatrix} \qquad \tilde{\beta} = \begin{bmatrix} 1 & 0 & 0 & 0 \\ 0 & 1 & 0 & 0 \\ 0 & 0 & -1 & 0 \\ 0 & 0 & 0 & -1 \end{bmatrix} = \begin{bmatrix} \tilde{1} & 0 \\ 0 & -\tilde{1} \end{bmatrix} \tag{71}$$

Note: for any vectors $\vec{A}$ and $\vec{B}$:

$$\tilde{\boldsymbol{\alpha}} \cdot \vec{\boldsymbol{A}} \tilde{\boldsymbol{\alpha}} \cdot \vec{\boldsymbol{B}} = \vec{\boldsymbol{A}} \cdot \vec{\boldsymbol{B}} + \boldsymbol{i} \tilde{\boldsymbol{\alpha}} \cdot (\vec{\boldsymbol{A}} \times \vec{\boldsymbol{B}}) \tag{72}$$

Dirac equation: non-relativistic limit I

Dirac equation in el.-mag. field ($\vec{E} = -\nabla\Phi(\vec{r}) = -\frac{1}{e}\nabla V(\vec{r})$):

$$i\hbar\frac{\partial\psi(\vec{r},t)}{\partial t} = \left(c\tilde{\alpha}\cdot\left(\frac{\hbar}{i}\nabla - e\vec{A}(\vec{r})\right) + \tilde{\beta}mc^2 + V(\vec{r})\right)\psi(\vec{r},t) \quad (73)$$

To take non-relativistic limit, we write

$$\psi(\vec{r},t) = \begin{bmatrix}\phi(\vec{r},t)\\ \chi(\vec{r},t)\end{bmatrix} \quad (74)$$

substituting $\tilde{\alpha}$ and $\tilde{\beta}$ from Eqs. (70-71)

$$i\hbar\frac{\partial}{\partial t}\begin{bmatrix}\phi(\vec{r},t)\\ \chi(\vec{r},t)\end{bmatrix} = \left(\frac{\hbar}{i}\nabla - e\vec{A}(\vec{r})\right)\cdot\tilde{\sigma}\begin{bmatrix}\chi(\vec{r},t)\\ \phi(\vec{r},t)\end{bmatrix} + \left(V(\vec{r}) \pm mc^2\right)\begin{bmatrix}\phi(\vec{r},t)\\ \chi(\vec{r},t)\end{bmatrix} \quad (75)$$

Dirac equation: non-relativistic limit II

Time dependence of $\psi(\vec{r},t)$:

$$\psi(\vec{r},t) = \psi(\vec{r}) \exp[-iWt/\hbar] \approx \psi(\vec{r}) \exp[-imc^2 t/\hbar] \qquad (76)$$

which is valid for both components of $\psi(\vec{r},t)$.
Substituting this time derivative of $\chi(\vec{r},t)$ into lower Eq. (75) and ignoring small terms, we get relation between $\phi(\vec{r},t)$ and $\chi(\vec{r},t)$

$$\chi(\vec{r},t) = \frac{1}{2mc}\left(\frac{\hbar}{i}\nabla - e\vec{A}(\vec{r})\right)\cdot\tilde{\sigma}\phi(\vec{r},t) \qquad (77)$$

Hence, for small speeds ($\vec{p} = m\vec{v}$, and $v \ll c$), $\chi(\vec{r},t)$ is much smaller than $\phi(\vec{r},t)$ by factor about v/c.

Dirac equation: non-relativistic limit III

Substituting $\chi(\vec{r},t)$ from Eq. (77), into upper Eq. (75)

$$i\hbar\frac{\partial}{\partial t}\phi(\vec{r},t) = \frac{1}{2m}\left(\left(\frac{\hbar}{i}\nabla - e\vec{A}(\vec{r})\right)\cdot\tilde{\sigma}\right)^2 \phi(\vec{r},t) + \left(V(\vec{r}) + mc^2\right)\phi(\vec{r},t) \tag{78}$$

Using $\tilde{\sigma}\cdot\vec{A}\tilde{\sigma}\cdot\vec{B} = \vec{A}\cdot\vec{B} + i\tilde{\sigma}\cdot(\vec{A}\times\vec{B})$

$$\begin{aligned}\left(\left(\frac{\hbar}{i}\nabla - e\vec{A}(\vec{r})\right)\cdot\tilde{\sigma}\right)^2\phi &= \left(\frac{\hbar}{i}\nabla - e\vec{A}(\vec{r})\right)^2\phi - e\hbar\tilde{\sigma}\cdot(\nabla\times\vec{A} + \vec{A}\times\nabla)\phi \\ &= \left(\frac{\hbar}{i}\nabla - e\vec{A}(\vec{r})\right)^2\phi - e\hbar\tilde{\sigma}\cdot\vec{B}\phi \qquad (79)\end{aligned}$$

And it leads to (see next slide)

Dirac equation: non-relativistic limit IV

$$i\hbar\frac{\partial}{\partial t}\phi(\vec{r},t) = \left(\frac{1}{2m}\left(\frac{\hbar}{i}\nabla - e\vec{A}(\vec{r})\right)^2 - e\hbar\tilde{\sigma}\cdot\vec{B} + V(\vec{r}) + mc^2\right)\phi(\vec{r},t) \tag{80}$$

- Results is Pauli equation, introducing the spin!
- magnetic moment (of electron) is predicted to be $\mu = e\hbar/(2m)$
- although proton and neutron have also spin 1/2, t does not predict their magnetic moment $\rightarrow$ problem is that they are composite particles.

Dirac equation: non-relativistic limit V

When Dirac equation is solved up to order $1/c^2$, we get

$$\begin{aligned}
\hat{H} =& \frac{1}{2m}\left(\frac{\hbar}{i}\nabla - e\vec{A}(\vec{r})\right)^2 + V(\vec{r}) + mc^2 \qquad (81) \\
& - e\hbar\tilde{\sigma}\cdot\left(\hat{\mathbf{B}} + \frac{\vec{E}\times\hat{\mathbf{p}}}{mc^2}\right) \qquad \text{(Zeeman term in } \bar{e} \text{ rest frame)} \\
& + \frac{e}{2mc^2}\hat{\mathbf{S}}\cdot(\vec{E}\times\hat{\mathbf{v}}) \qquad \text{Spin – orbit coupling} \\
& - \frac{1}{8m^3c^2}(\vec{p} - e\vec{A})^4 \qquad \text{Special relativity energy correction} \\
& + \frac{\hbar^2 e}{8m^2c^2}\nabla^2 V(\vec{r}) \qquad \text{Darwin term}
\end{aligned}$$

Darwin term: electron is not a point particle, but spread in volume of size of Compton length $\approx \hbar/mc$.

Free particle and antiparticle

Solving Dirac equation for free particle

$$\hat{\boldsymbol{H}} = \boldsymbol{c}\tilde{\boldsymbol{\alpha}} \cdot \hat{\mathbf{p}} + \tilde{\boldsymbol{\beta}}\boldsymbol{m}\boldsymbol{c}^{\mathbf{2}} \qquad (82)$$

Solution of free particle ($U(\vec{p}$ has four dimensions)

$$\psi = U(\vec{p}) \exp[i(\vec{p} \cdot \vec{r} - Wt)/\hbar] \qquad (83)$$

Substituting in Dirac equation Eq.(82), and assuming motion in xy plane ($p_z = 0$), we get

$$\begin{bmatrix} mc^2 - W & 0 & 0 & cp_- \\ 0 & mc^2 - W & cp_+ & 0 \\ 0 & cp_- & -mc^2 - W & 0 \\ cp_+ & 0 & 0 & -mc^2 - W \end{bmatrix} \begin{bmatrix} U_1 \\ U_2 \\ U_3 \\ U_4 \end{bmatrix} e^{i\vec{p}\cdot\vec{r}/\hbar} = 0 \qquad (84)$$

Outline

Spin and charge current

- spin current densities $j_\uparrow$ and $j_\downarrow$ may be different
- both can be carries by electrons and holes

Charge current

- $j_{\mathrm{ch}} = j_\uparrow + j_\downarrow$
- transfer of charge
- scalar quantity

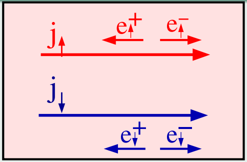

Spin current

- $j_{\mathrm{sp}} = j_\uparrow - j_\downarrow$
- transfer of angular momentum $\vec{L}$
- vectorial quantity

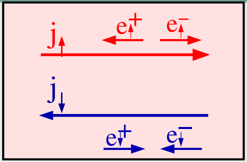

Diffusion equation of spin-polarized current

$$j_{\uparrow/\downarrow} = \frac{\sigma_{\uparrow/\downarrow}}{e}\frac{\partial \mu}{\partial x} \tag{85}$$

$$\frac{\partial^2(\mu_\uparrow - \mu_\downarrow)}{\partial x^2} = \frac{\mu_\uparrow - \mu_\downarrow}{\lambda_{sf}^2} \tag{86}$$

$$\frac{\partial^2(\sigma_\uparrow\mu_\uparrow + \sigma_\downarrow\mu_\downarrow)}{\partial x^2} = 0 \tag{87}$$

Spin-injection from FM

How to create spin current $j_{\rm sp}$ in non-FM?

$\Rightarrow$ there are several ways of spin-injection, but here we discuss only spin injection by charge current flow from FM (spin injection).

Local spin-injection:

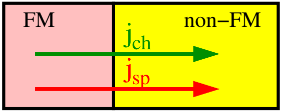

non-FM contains nonzero both:

- spin current $j_{\rm sp} = j_\uparrow - j_\downarrow$
- charge current $j_{\rm ch} = j_\uparrow + j_\downarrow$

Non-local spin-injection:

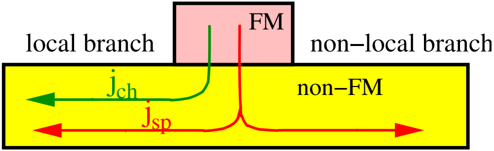

- $j_{\rm ch}$ is driven from FM to local branch of non-FM
- $j_{\rm sp}$ diffuses from FM to both local and non-local branches of non-FM

Two current model for local spin injection

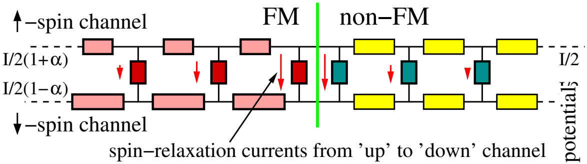

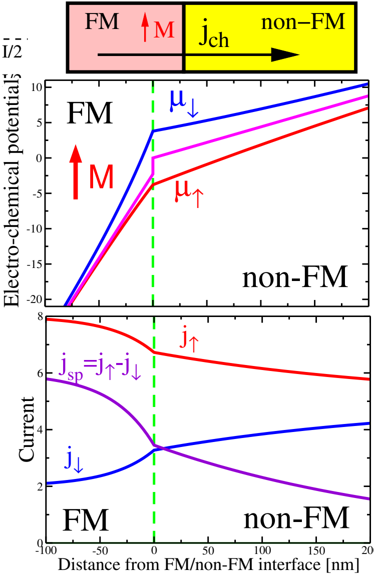

- two current model consist of resistances of ↑, ↓ channels and of shortcutting resistances between both channels.
- FM has different resistivities for ↑ and ↓ channels ⇒ (i) Both channels hold different currents $j_\uparrow$, $j_\downarrow$. (ii) Spin relaxing current αI has to relax from ↑ to ↓ channel.
- The spin relaxing current αI (i) relaxes partly in both FM and non-FM material. (ii) creates $\Delta\mu = \mu_\uparrow - \mu_\downarrow$ on the interface.

Simplified two current model

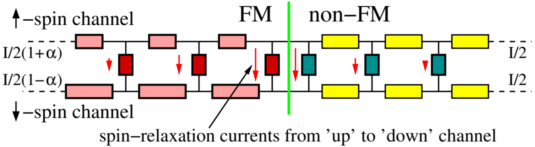

→ All shortcutting resistances can be expressed by one spin resistance R_λ, expressing all relaxations.

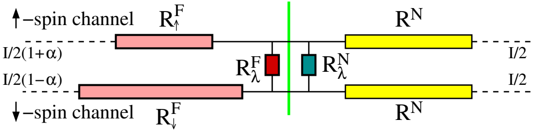

Spin resistances R_λ^F, R_λ^N:

$$R_\lambda^F = \frac{\lambda_F}{\sigma_F S}\left(\frac{1}{1-\alpha^2}\right)$$

$$R_\lambda^N = \frac{\lambda_F}{\sigma_F S}$$

S : cross-sectional area

λ : spin-diffusion length

σ : conductivity

$\alpha = \frac{\sigma_\uparrow - \sigma_\downarrow}{\sigma_\uparrow + \sigma_\downarrow}$: spin polarization

Spin injection efficiency

The spin relaxing current αI relaxes in both FM and non-FM

Ineffective spin injection: $R_\lambda^F \ll R_\lambda^N$ (Conduction mismatch)

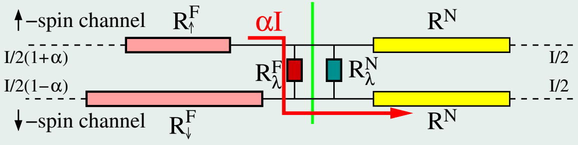

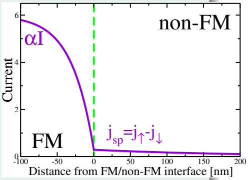

Effective spin injection: $R_\lambda^F \gg R_\lambda^N$

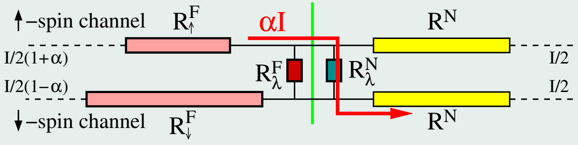

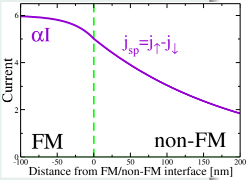

Values of spin resistances R_λ

$$R_\lambda^F = \frac{\lambda_F}{\sigma_F S}\left(\frac{1}{1-\alpha^2}\right)$$

	σ $[\Omega^{-1}\text{m}^{-1}]$	λ [nm] (RT)	α	R_λ $[\Omega]$ $(S = 10^4\ \text{nm}^2)$
Py	7.3×10^6	4	0.7	0.11
Co	4.2×10^6	40	0.36	0.98
Cu	48×10^6	350	0	0.72
Al	31×10^6	600	0	1.90
GaAs	500	2000	0	4×10^5

- usually: $R_\lambda^F \ll R_\lambda^N$
  $\Rightarrow$ poor spin injection!
  $\rightarrow$ very poor for semiconductor (solved by Schottky barrier)

Non-local spin injection

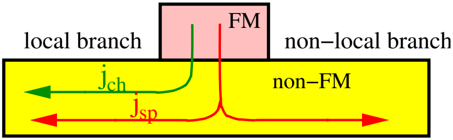

- j_{ch} is driven from FM to local branch of non-FM
- j_{sp} diffuses from FM to both local and non-local branches of non-FM

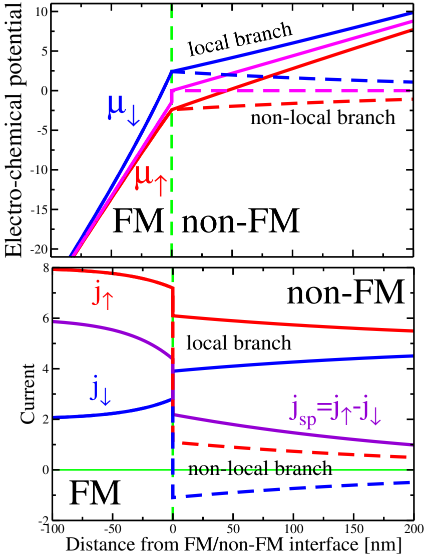

Outline

Magnetotransport

Dependence of conductivity on magnetization state.
Various effects were discovered:

- Giant magnetoresistance (GMR).
- Tunnel magnetoresistance (TMR).
- Ballistic magnetoresistance (BMR).
- Anisotropic magnetoresistance (AMR).
- Colossal magnetoresistance (CMR).

Applications:

- magnetic sensors (information recording, new memories, medical applications, etc.).
- quantized conductivity – metrology.

Example - Hard disc principle I

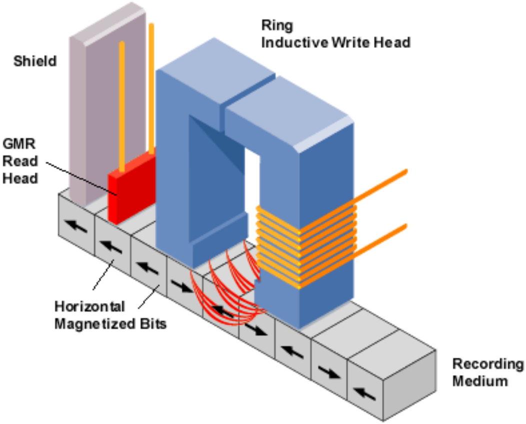

http://encyclopedia2.thefreedictionary.com/Magnetoresistance

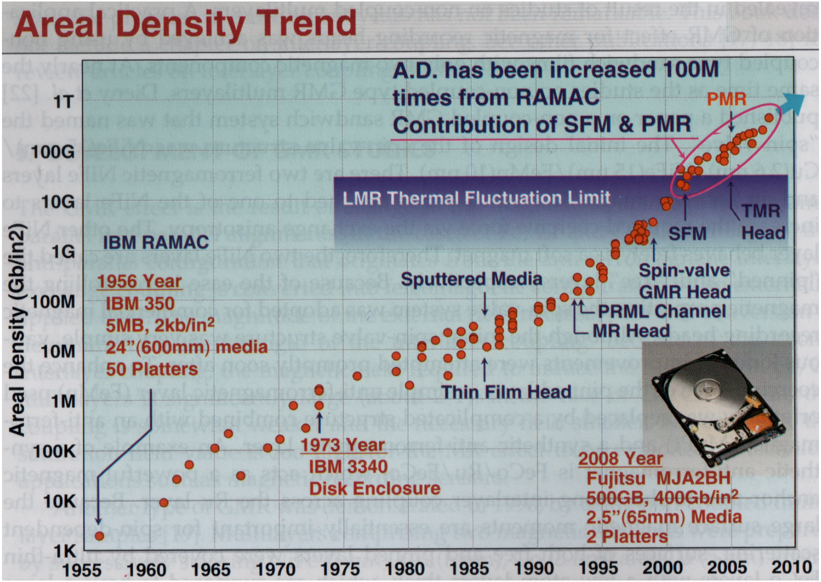

T. Shinjo, Nanomagnetism and Spintronics

Giant magnetoresistance (GMR)

Change of resistivity when between parallel (P) and antiparallel (AP) state

$$\mathrm{MR} = \frac{R_{AP} - R_P}{R_P}$$

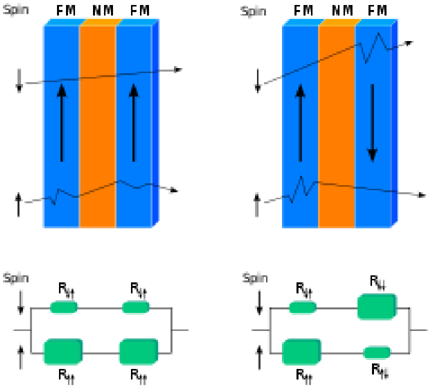

image: wikipedia

Giant magnetoresistance (GMR)

Example of GMR FM bilayer simple stacking:

- Co/Cu/NiFe: GMR stack itself.
- antiferromagnetic (AFM) pinning: pinning of Co layer by AFM FeMn.
- cap layer: protection against oxidation.
- buffer layer: to improve crystallographic growth.

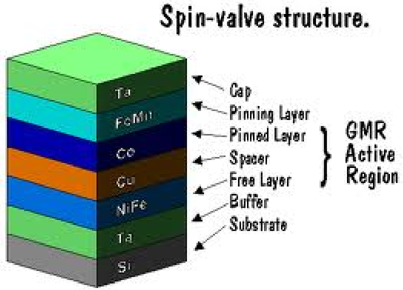

http://www.stoner.leeds.ac.uk/Research/TutGMRSpin

Giant magnetoresistance (GMR)

Example of more complex GMR stacking:

- interface engineering: thin $Co_{0.9}Fe_{0.1}$: improvement of spin polarization and/or spin scattering at the interface.
- permalloy $Ni_{0.8}Fe_{0.2}$: small coercivity of free FM layer.
- pinning of fixed FM layer by AFM $Ir_{0.2}Mn_{0.8}$.
- artificial AFM coupling: two $Co_{0.9}Fe_{0.1}$ layers AFM coupled by Ru(0.6): to vanish stray field from pinned FM layer acting on free FM layer (i.e. removing magnetic bias).

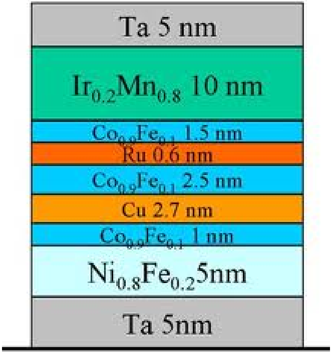

http://www.nist.gov/pml/electromagnetics/magnetic

Giant magnetoresistance (GMR)

- Original GMR work (A. Fert) done for $(Fe/Cr)_N$ stack.

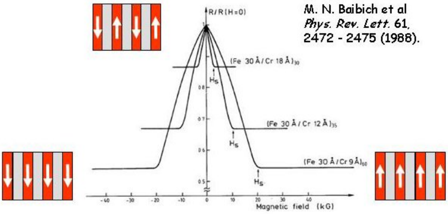

- Fe/Cr/Fe can be AFM coupled (example for NiCo/Ru/NiCo).

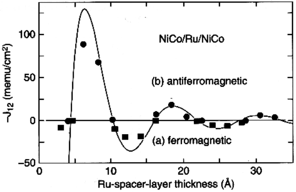

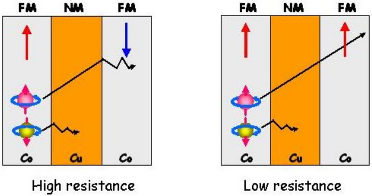

image: wikipedia

Typology of used GMR

According to coupling of the FM layers:

- GMR in exchange coupling layers: FM layers coupled by exchange. May consists of many FM layers (for example $(\text{Fe/Cr})_N$ stack).
- non-coupling GMR: two free FM layers.
- spin-valve GMR: one FM is fixed by AFM coupling, second FM layer is free.
- Granular GMR: nanoparticles of FM material (e.g. Fe, Co) are randomly spread inside non-FM metals (e.g. Cu, Ag).

According current direction (geometry):

- current-perpendicular-to-the-plane: CPP
- current-in-the-plane: CIP

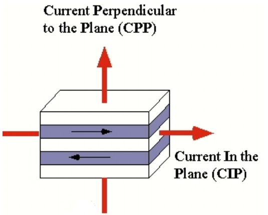

Theoretical description of GMR

- Simple conductivity model:

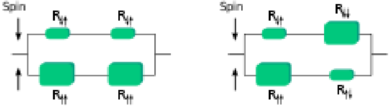

$$\mathrm{MR} = \left(\frac{\rho_\uparrow - \rho_\downarrow}{\rho_\uparrow + \rho_\downarrow}\right)^2 = \left(\frac{1-\alpha}{1+\alpha}\right)^2$$

where $\alpha = \rho_\downarrow / \rho_\uparrow$

- Two-channel Valet-Fert model (added spin accumulation, spin flipping, diffusive transport etc.):
[picture to be added]
- Spin-dependent resistivity of the interface due to:
  1. interfacial roughness: interfacial roughness and intermixing (alloying) of atoms cause additional spin scattering of electrons at interfaces.
  2. band matching at interfaces (see next two slides).

GMR: (ii) Band matching or mismatching at interfaces.

- Essence of the origin of electrical resistivity is the absence of translational invariance along the current direction because electrons' momentum may be not conserved.
- Interface for CPP geometry always breaks symmetry of the crystal.
- Band matching/mismatching of electron momentum (i.e. of electron's k-vector at Fermi surface) between both metals at the interface can reduce/increase effect of the interface resistance.
- There can be different band matching for spin-up and spin-down electrons $\Rightarrow$ spin-dependent interfacial resistivity can appear.
- For example Co/Cu has better match for $\uparrow$ electrons, but Fe/Cr has better match for $\downarrow$ electrons.

GMR: Band matching or mismatching at interfaces.

Fermi surfaces of Cr, Fe and Co:

Cr-bcc | Fe-bcc | Co-fcc

up

down

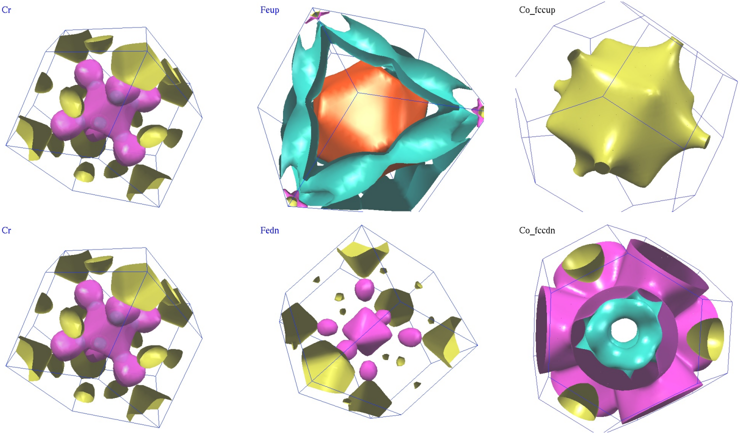

Tunnel magnetoresistance (TMR)

- Two FM layers are separated by non-conducting (insulator) layer.
- As insulator layer is very thin (about 1 nm), conduction electrons can tunnel through it.
- Different tunneling probability for P and AP configuration ⇒ TMR appears.

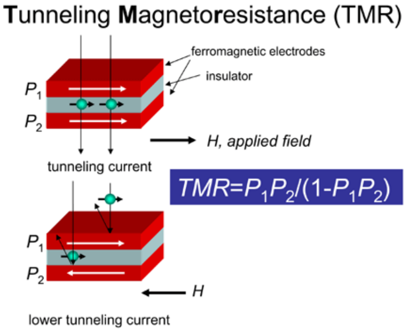

http://www.nims.go.jp/apfim/TMR.html

Diffusive tunneling:

- disorder at interface or amorphous barrier ⇒ breaks translation symmetry in parallel direction ⇒ $k_{\parallel}$ not conserved
- typical (most used diffusive tunnel barrier) is AlO_x barrier.
- amorphous tunnel barrier ⇒ Density of States (DOS) does not exist (does not have meaning) for the barrier.
- schematic energy diagram:

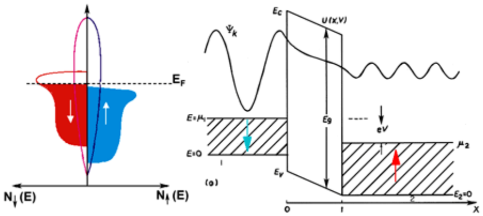

Tunneling probability is spin-dependent between split bands of 2 ferromagnets

https://www1.hitachigst.com/hdd/research/recording_head/cpp/index.html

Diffusive tunneling

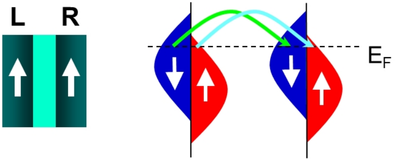

$$G_P \propto n_L^{\uparrow} n_R^{\uparrow} + n_L^{\downarrow} n_R^{\downarrow}$$

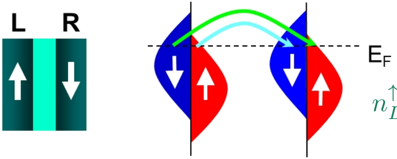

$$G_{AP} \propto n_L^{\uparrow} n_R^{\downarrow} + n_L^{\downarrow} n_R^{\uparrow}$$

http://physics.unl.edu/˜tsymbal

Julliere model:

$$\mathrm{TMR} \equiv \frac{G_{AP} - G_P}{G_{AP}} = \frac{2P_L P_R}{1 - P_L P_R}$$

$$P_L = \frac{n_L^{\uparrow} - n_L^{\downarrow}}{n_L^{\uparrow} + n_L^{\downarrow}} \qquad P_R = \frac{n_R^{\uparrow} - n_R^{\downarrow}}{n_R^{\uparrow} + n_R^{\downarrow}}$$

G_{AP}, G_P: antiparallel, parallel conductance of TMR structure

P_L, P_R: spin polarization of left, right ferromagnet

$n_L^{\uparrow/\downarrow}$, $n_R^{\uparrow/\downarrow}$: density of states at Fermi level for left (L), right (R) FM layer, for majority (↑) and minority (↓) electronds. I.e., number of electrons on Fermi level.

Jullière model (1975):

$$\mathrm{TMR} = \frac{2P_1P_2}{1 - P_1P_2}$$

- Originally assuming that TMR is effect of metal spin-polarization P_i.
- Later found that TMR also effected by:
  - chemical bonding on interface,
  - spin-dependent tunneling matrix elements (i.e. different electrons tunnel with different probability depending on initial and final electron state).
  - spin filtering (?).
  - details of structure of the tunnel barrier.
  - structure of the interface.
- Nowdays, diffusive tunnel barrier (AlO$_x$ barrier) were overcome by specular tunneling (MgO barrier).
- Nowdays, AlO$_x$ barrier used to measure spin-polarization of materials and tunneling spectroscopy (together with Andreev reflection, i.e. FM/superconductor junction).

Specular tunneling:

- barrier has the same translation symmetry as FM electrodes (epitaxial growth of the barrier - e.g. MgO barrier) $\Rightarrow k_{\|}$ can be preserved $\Rightarrow$ when symmetry of the wavefunction is the same for both FM electrodes, the probability of electron tunneling may increase substantially $\Rightarrow$ large tunneling for P state and small for AP state (e.g. TMR=1500%).

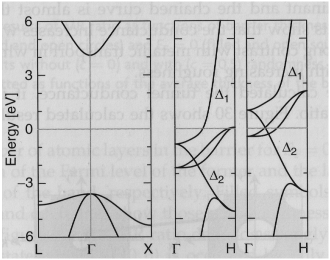

MgO, Fe-up, Fe-down

Specular tunneling

- Different tunneling probabilities for electrons from different bands in Fe/MgO/Fe structure for majority (up figure) and minority (bottom figure) electrons (Butler et al. PRB 63, 054416 (2001)).

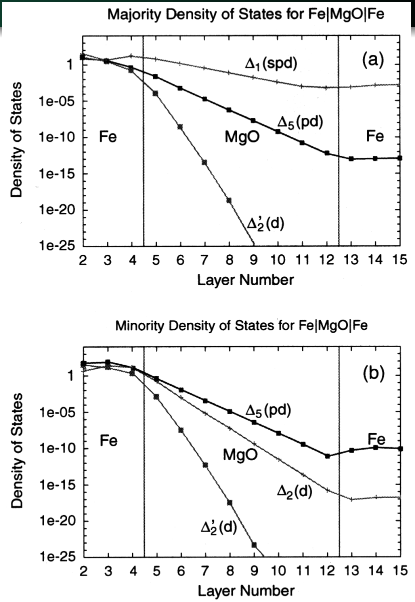

Difference between diffusive and specular tunneling:

"In the conventional MTJ devices, AlO_x making up the tunnel barrier material is an amorphous material with disordered atomic arrangement. As current flows, electrons are scattered in the tunnel barrier to lose the coherency of wave nature. On the other hand, in the novel TMR devices, MgO in the tunnel barrier is a crystalline material with atoms regularly arranged, and it has been theoretically predicted that when a current flows, electrons transport across the tunnel barrier keeping the coherency of the wave nature without being scattered. According to W.H. Butler, 2001, it is an essential requirement for huge magnetoresistance to appear that electrons propagate across the tunnel barrier while the coherency of their wave functions is conserved."

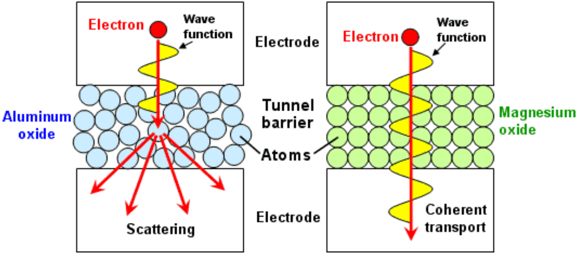

http://www.aist.go.jp/aist_e/latest_resear

Specular tunneling: oscillations

Dependence of TMR in Fe/MgO/Fe as function of MgO thickness. The TMR shows local maximum/minimum values for the MgO thicknesses shown with red/blue arrows, respectively. The mechanism of this phenomenon is related to the coherency of tunneling electrons. Within the MgO tunnel barrier, the electron wave has a particular periodicity. It is theoretically predicted that when MgO contains an integral multiple (1, 2, 3,. . .) of periodicity the magnetoresistance is smaller, and when it includes an integral multiple plus a half (1.5, 2.5, 3.5, . . .), the resistance is greater. That is, the present observation of periodic changes in magnetoresistance constitutes a direct evidence of electron propagation within the device while keeping the coherency of the wave nature. This is the first experimental proof of the mechanism of huge magnetoresistance based on the coherent electron tunneling."

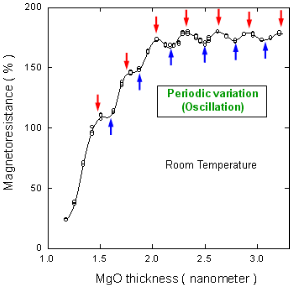

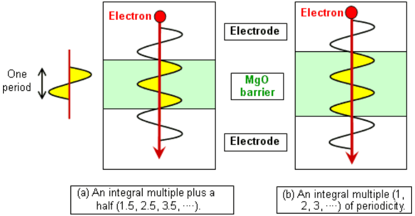

http://www.aist.go.jp/aist_e/latest_research/2004/20041124/2004112

TMR comparison of diffusive and specular tunneling

- specular tunneling can be much larger than diffusive tunneling.

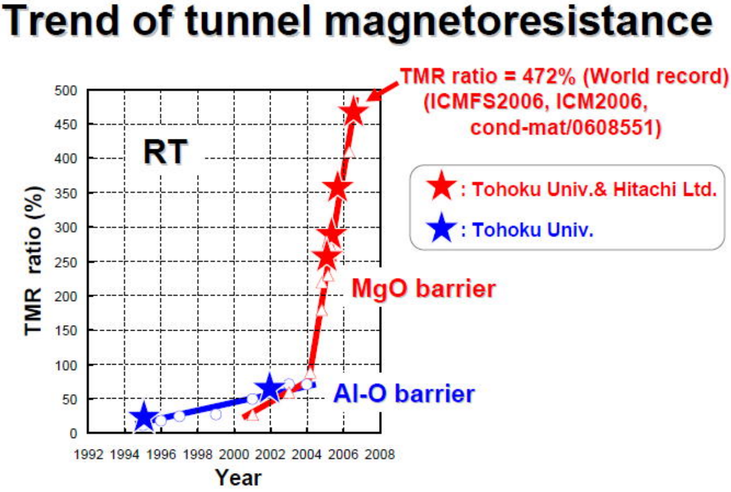

http://www.ohno.riec.tohoku.ac.jp/english/Research_toptst-file/MRAM/MRAM.html

Specular tunneling: large dependence on temperature

- TMR strongly decreases with increasing temperature:

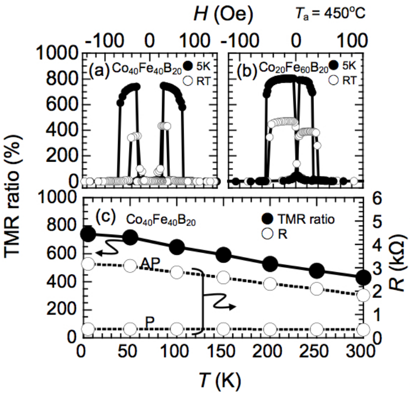

Fig. 2. Magnetoresistance loops of pseudo spin-valve $Co_{40}Fe_{40}B_{20}$/MgO/$Co_{40}Fe_{40}B_{20}$ MTJs (a) and $Co_{20}Fe_{60}B_{20}$/MgO/$Co_{20}Fe_{60}B_{20}$ MTJs (b) at room temperature (open circles) and 5 K (solid circles). MTJs were annealed at 450°C. TMR ratios are as high as 450% at RT and 747% at 5 K for MTJ with $Co_{40}Fe_{40}B_{20}$ electrodes and 472% at RT and 804% art 5 K for one with $Co_{20}Fe_{60}B_{20}$ electrodes. (b) Temperature dependence of resistance (open circles) and TMR ratio (solid circles) in parallel and anti-parallel configurations in the $Co_{40}Fe_{40}B_{20}$/MgO/$Co_{40}Fe_{40}B_{20}$ MTJ.

J. Hayakawa et al., http://arxiv.org/ftp/cond-mat/papers/0610/0610526.pdf

Specular tunneling: large dependence on temperature

- TMR strongly decreases with increasing temperature:

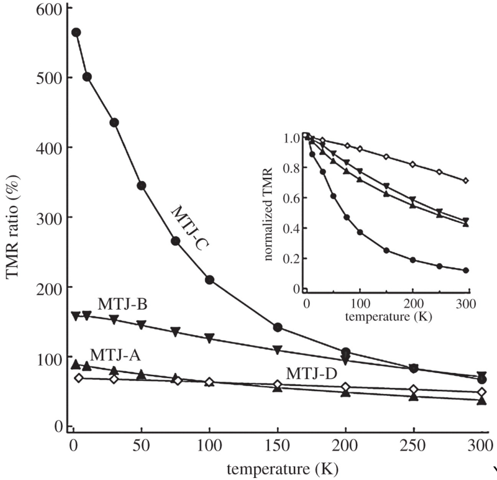

Y. Sakuraba et al.

Outline

Spin-torque (simple picture) I

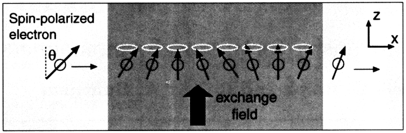

[S. Maekawa, Concepts in spin-electronics]

One passing electron:

- spin-polarized electron from non-FM enters FM material.
- (1) spin-up electrons have larger transmission amplitude through the interface than down-electron (e.g. for Cu/Co). Hence, the relative amplitudes of the spin-up and spin-down will be changed ⇒ the transmitted spin is less tilted (smaller θ) compared to the initial tilt.
- (2) Due to huge exchange field, electrons starts to precess quickly (on a short scale).
- as angular moment must be conserved, the moment of the FM must precess about the spin.

Spin-torque (simple picture) II

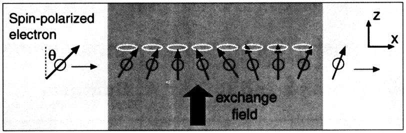

[S. Maekawa, Concepts in spin-electronics]

Many electrons:

- as precession is very quick (about several precession by 1nm of FM), the outgoing phase of electrons is 'random' (as incoming electrons has different $\vec{k}$-vectors, different speeds, etc).
- hence, by summing over many electrons, only z-component of electron momentum persists
  $\Rightarrow$ x-component (so-called transverse component) of angular momentum is passed to FM material
  $\Rightarrow$ magnetization of FM is tilted in direction of the incoming spin (or this angular moment can generate spin-waves).
- spin-torque transfer is like interface effect (less than 1 nm depth).

Spin-torque (simple picture) III

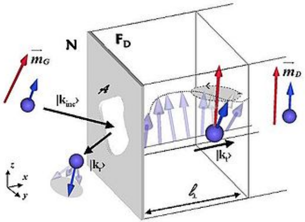

[fr.wikipedia.org/wiki/Transfert_de_spin]

Neglected effects:

- neglected reflection of electrons at interfaces.
- some angular moment will be transfered also by reflecting electrons.

However, in any case,

- FM absorbs transverse component of the incoming spin angular momentum.
- FM magnetic moment will feel torque towards incoming spin polarization.

Spin-torque – two FM layers

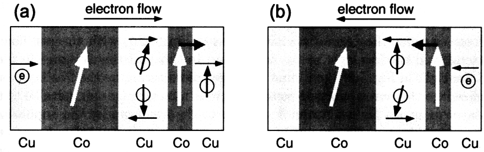

[S. Maekawa, Concepts in spin-electronics]

- assumed system has two FM layers: FM-fixed / non-FM / FM-free.
- Key feature: asymmetry of the spin-transfer effect with respect to the current direction.

Spin-torque – two FM layers – negative current

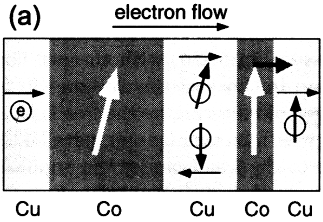

[S. Maekawa, Concepts in spin-electronics]

- electrons flow from FM-fixed towards FM-free.
- electrons get polarized by FM-fixed. Then pass to FM-free, transmitting angular moment to it (as discussed above) $\Rightarrow$ torque to FM-freer to stabilize parallel alignment.

Spin-torque – two FM layers – positive current

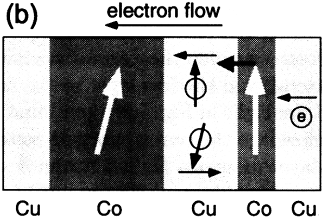

- electrons flow from FM-free towards FM-fixed.
- electrons get polarized by FM-free and moment is transfered to FM-fixed. However, we assume FM-fixed to be fixed, hence, nothing happens to FM-fixed.
- However, part of the electrons incoming to FM-fixed is reflected.
- As transmittance is higher for up-electrons, reflected electrons are mostly down-electrons (i.e. *anti-parallelly* polarized with respect to FM-fixed).
- those reflected electrons are absorbed by FM-free ⇒ torque to FM-freer to stabilize anti-parallel alignment.

Spin-torque – two FM layers

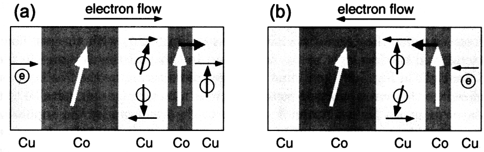

[S. Maekawa, Concepts in spin-electronics]

- Key feature: asymmetry of the spin-transfer effect with respect to the current direction.
- initial state of FM-free is not important,
  $\rightarrow$ negative current (a) stabilizes parallel alignment.
  $\rightarrow$ positive current (a) stabilizes anti-parallel alignment.
- above is valid for FM material of FM-fixed, when it is positive polarizer (i.e. preferentially transmitting majority (up) electrons), such as Co.
- when FM-fixed is negative polarizer (such as FeCr or NiCr), negative current (a) stabilizes antiparallel alignment and *vica-versa*.

Landau-Lifshitz equation (without damping)

magnetization dynamics (without damping) is described by

$$\frac{\partial \vec{M}}{\partial t} = -\frac{g\mu_B}{\hbar}\vec{M} \times \vec{B}$$

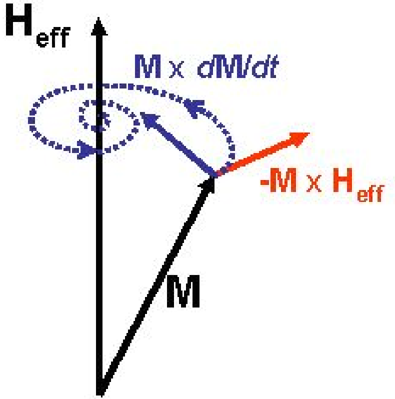

Landau-Lifshitz equation (with damping)

magnetization dynamics (with damping) is described by

$$\frac{\partial \vec{M}}{\partial t} = -\frac{g\mu_B}{\hbar}\vec{M} \times \vec{B}_{\rm eff} + \frac{\alpha}{M_S}\vec{M} \times \frac{\partial \vec{M}}{\partial t}$$

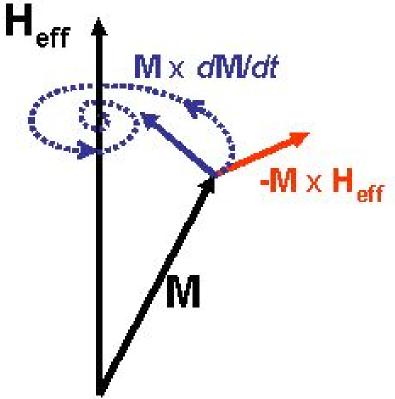

Landau-Lifshitz equation (with spin-torque term)

magnetization dynamics (with damping and spin-torque) is:

$$\frac{\partial \vec{M}}{\partial t} = -\frac{g\mu_B}{\hbar}\vec{M}\times\vec{B}_{\text{eff}} + \frac{\alpha}{M_S}\vec{M}\times\frac{\partial \vec{M}}{\partial t} + \frac{\gamma\hbar}{2e}\frac{\eta J}{M_S^2 d}\vec{M}\times(\vec{M}\times\vec{p})$$

- p: direction of spins in the injected spin-current.
- spin-torque term has the direction as damping term, but its sign depends on current direction

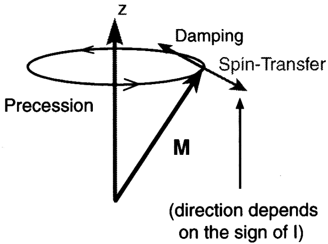

When value of spin-torque compared to damping has:

- the same direction, damping is stronger (stabilization).
- opposite direction, magnetization reversal.
- opposite and the same strength: permanent precession (oscillator)

Spin transfer

The loss of transverse spin angular momentum at the normal metal-ferromagnet interface is therefore

$$[\vec{p} - (\vec{p} \cdot \vec{m})\vec{m}]/(2e),$$

$\vec{m}$: normalized magnetization. $\vec{m} = 1$.
The torque has to be shared with all magnetic moments $M_s V$ of the ferromagnetic of the film with volume V

$$T_{STT} = \left(\frac{\partial \vec{m}}{\partial t}\right)_{STT} = \frac{1}{M_s V}\left(\frac{\partial \vec{m} M_s V}{\partial t}\right)_{STT} = -\frac{\gamma \hbar}{2e M_s V}(\vec{m} \times (\vec{m} \times \vec{p}))$$

where vector identity BAC-CAB was used;
$\vec{a} \times (\vec{b} \times \vec{c}) = \vec{b}(\vec{a} \cdot \vec{c}) - \vec{c}(\vec{a} \cdot \vec{b})$.

Correct handling of dynamics of FM-free

Spin current may generate instability of the magnetization state of FM-free. To correctly described, all forces acting on $\vec{M}$ must be handled:

- spin-torque.
- external magnetic field.
- Oersted field ($\vec{H}$ generated by current).
- dipolar field ($\vec{H}$ from other FM layers).
- anisotropies (shape and magnetocrustalline).
- damping.
- thermal fluctuation

Often used approximation: $\vec{M}$ in FM-free acts as spinor, i.e. as monodomain state.

Sample geometries to study spin-transfer

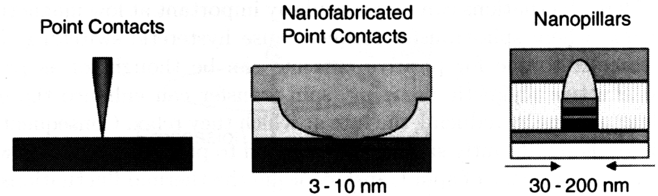

Small devices needed (about 100 nm in diameter, few nm thickness) as:

- spin-torque ($\sim I/V$) overcomes Oersted field ($\sim I/S$) (?).
  $\rightarrow$ also, Orsted field prefers vortex magnetization state.
- monodomain state of FM-free is kept.
- critical currents are in order of mA.
- small device better disposes heat.

Most often studied system are nanopillars (well defined, small critical current density, tuning possibilities, well-defined anisotropy (elliptical shape)).

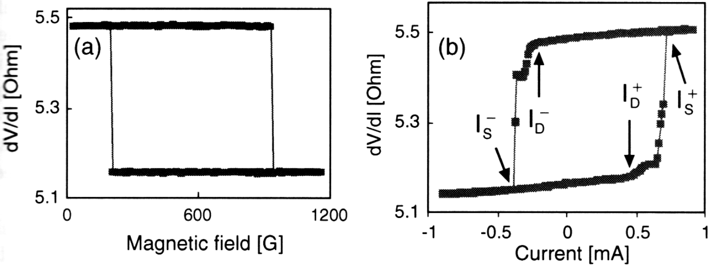

FIG. 5.5. (a) Switching of the magnetic layers in a nanopillar device between parallel and antiparallel orientations, driven by a magnetic field at 4.2 K. (b) Switching in the same device, driven by spin-transfer torques from an applied current at 4.2 K. The current can excite a precessional excitation at the current I_D, prior to full magnetic reversal at I_S.

Py(2nm)/Cu(6nm)/Py(20nm)

- (a) field offset due to FM-fixed dipolar field
- (b) external field sets to compensate field offset. Then, switching P↔AP states by passing current.

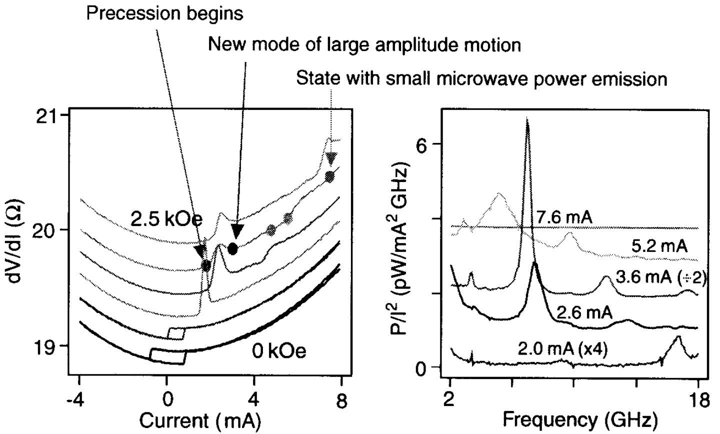

FIG. 5.6. Left: differential conductance of a nanopillar device for applied magnetic fields from 0 Oe to 2.5 kOe, at increments of 0.5 kOe. Right: microwave power spectra measured at 2 kOe, for selected values of current. The spectra are offset vertically. Different magnitudes of current excite different types of dynamical magnetic modes.

- Co(3nm)/Cu(10nm)/Co(40nm)
- small field $\rightarrow$ only reversal by current.
- larger field $\rightarrow$ no hysteresis switching, turning on/off dynamical modes (oscillation modes).
- smallest current (here 2 mA) provides small angle precession (FMR).
- larger current provides large angle-precession (frequency reduces).

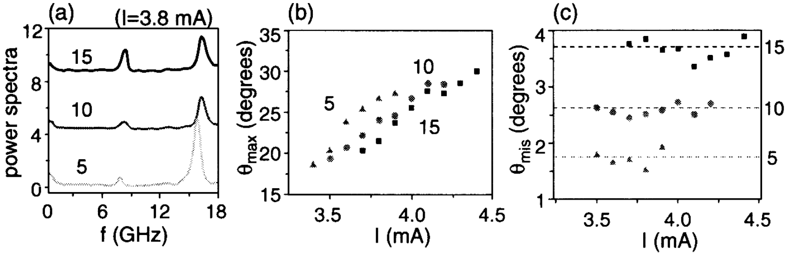

FIG. 5.7. Variation of microwave signals as a function of the angle of the applied magnetic field, for a field magnitude of 700 G, for a sample with an etched free layer and a continuous (un-etched) fixed layer. (a) The relative magnitudes of the first and second harmonics are different when the magnetic field is applied 5, 10, and 15 degrees from the easy axis of the free layer. (b and c) From the relative magnitude of the harmonics, we calculate the amplitude of the precessional motion ($\theta_{\max}$) and the average angle of misalignment between the fixed and free layer moments (θ_{mis}) using Eqs (5.1) and (5.2). These measurements demonstrate that the microwave signals originate from the GMR effect, not inductive signals.

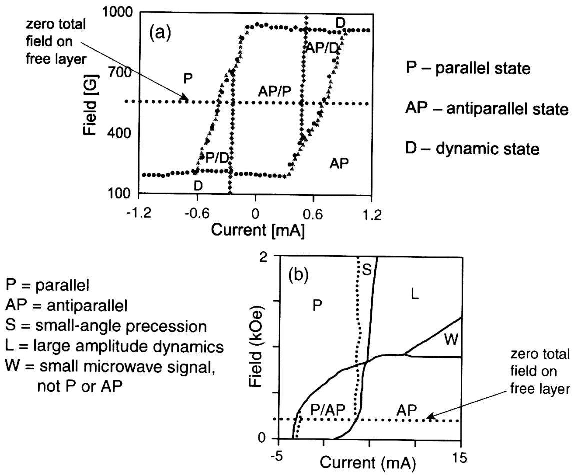

FIG. 5.8. (Top) phase diagram illustrating the different magnetic configurations as a function of current and applied magnetic field for a nanopillar with a permalloy free layer, at 4.2 K. Regions with two labels indicate hysteresis. (Bottom) phase diagram over a larger range of current and field for a nanopillar sample with a cobalt fixed layer, at room temperature.

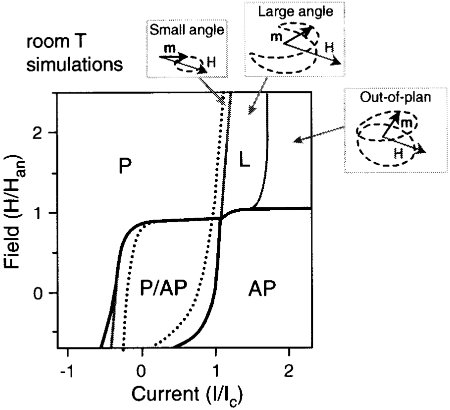

FIG. 5.9. Calculated dynamical phase diagram for parameters corresponding to a single-domain cobalt free layer at room temperature. (Compare to Fig. 5.8.) The Landau–Lifshitz–Gilbert simulation gives an accurate description of the existence and relative positions of the parallel, antiparallel, and dynamical states. However, there are differences at large currents which may indicate departures from single-domain behavior.

Spin-pumping I

"Spin pumping by a precessing ferromagnet is, in some sense, the reverse process of current-induced magnetization dynamics. When the pumped spin angular momentum is not quickly dissipated to the normal-metal atomic lattice, a spin accumulation builds up and creates reaction torques due to transverse-spin backflow into ferromagnets."

Y. Tserkovnyak, Rev.Mod. Phys. 77, 1375 (2005)

- FM/NF interface.
- FM layer precesses.
- spin-current is pumped to NF.
- non-local behavior of magnetization damping (damping is spread to NF).

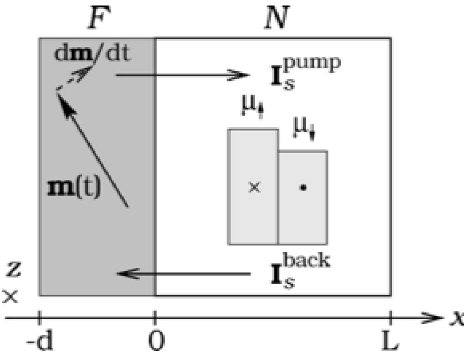

Spin-pumping II

Spin current pumped to NF layer:

$$\mathbf{I}_s^{\text{pump}} = \frac{\hbar}{4\pi}\left(A_r \mathbf{m} \times \frac{d\mathbf{m}}{dt} - A_i \frac{d\mathbf{m}}{dt}\right)$$

- $\vec{m}$: relative magnetization.
- $A = A_r + iA_i = g^{\uparrow\downarrow} - t^{\uparrow\downarrow}$; A: complex spin-pumping conductance, $g^{\uparrow\downarrow}$: interfacial mixing conductance, $t^{\uparrow\downarrow}$: transmission mixing conductance.
- for thick FM layer, $A = g^{\uparrow\downarrow}$.

$$\mathbf{I}_s^{\text{back}} = \frac{1}{2\pi}\left(g_r^{\uparrow\downarrow} \boldsymbol{\mu}_s + g_i^{\uparrow\downarrow} \mathbf{m} \times \boldsymbol{\mu}_s\right)$$

$$= \frac{\hbar}{4\pi}\left(g_r^{\uparrow\downarrow} \mathbf{m} \times \frac{d\mathbf{m}}{dt} - g_i^{\uparrow\downarrow} \frac{d\mathbf{m}}{dt}\right)$$

- μ_s:spin accumulation in NF
- $\mu_s = \hbar/2(\vec{m} \times d\vec{m}/dt)$
- $\mu_s \equiv \Delta\mu = \hbar\omega$

Spin pumping III

Spin torque and spin pumping are inverse effects:

- spin torque: spin currents cause torque on magnetization and hence its moves (transfer of angular momentum from electrons to magnetization).
- spin pumping: moving magnetization cause generation of spin current (moving magnetization is changing its angular momentum and hence it is transferred to itinerant electrons).

Spin pumping:

- causes increase of magnetic dumping as the losing angular momenta is also transferred to adjacent layers.
- simple way to create pure spin-current in non-FM layer. But the spin of electrons is precessing, causing effective smaller spin-diffusion length due to dephasing of their precession (Hanle effect).

Spin-pumping: experiment in Py/Cu(d)/Pt

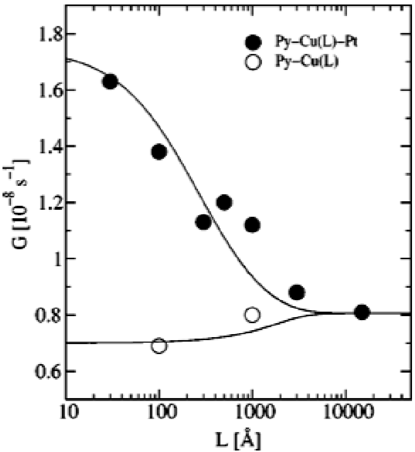

FIG. 5. Circles show the measurements by Mizukami *et al.* (Ref. 16) of the Gilbert damping in Py-Cu-Pt trilayer and Py-Cu bilayer as a function of the Cu buffer thickness L. Solid lines are our theoretical prediction according to Eqs. (26) and (27).

- measured Gilbert damping G in Py/Cu(d)/Pt system.
- Cu is like good spin conductor, Pt is like spin-damper.
- with increasing Cu thickness, the damping changes, due to different spin-current damped by Pt layer.

Spin-torque oscillators

Single oscillator (frequency controlled by value of current)

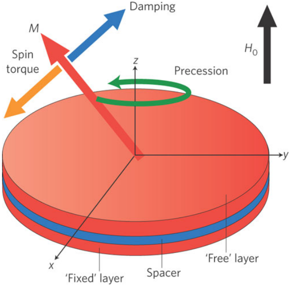

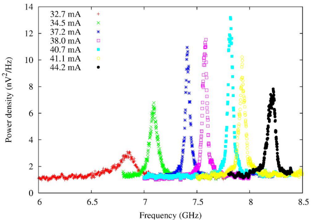

Co90Fe10(1.5nm)/Py(2nm) free layer / exchange-biased Co90Fe10(3.5nm)

http://www.imec.be/tunamos

- frequency can be adjusted by value of passing current
- single oscillator has too small power $\Rightarrow$ coupling several oscillators together

Spin-torque oscillators

Coupling of several oscillators increases outgoing power. Coupling by:

- dipolar field.
- by spin-waves of shared fixed FM layer.
- only by electrical current (simplest way).

Domain wall dynamics

Pushing domain wall by:

- external field.
- spin current.

Pushing domain wall by spin current:

Types of domain walls (Bloch and Neel domain walls):

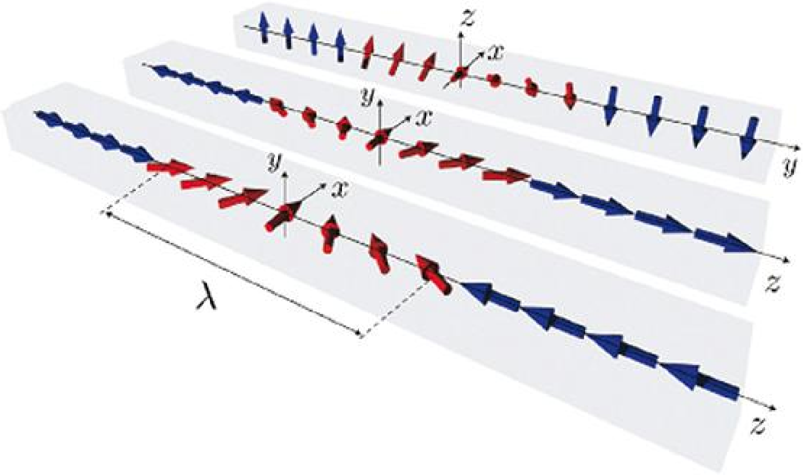

Domain wall types in FM wire for in-plane systems

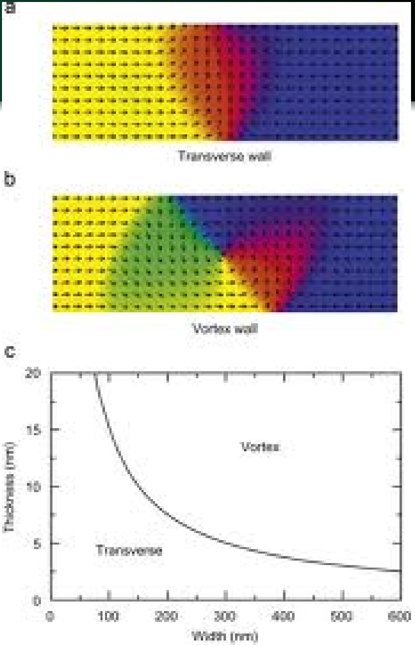

Domain wall (DW) speed

- Py wire, 20 nm-thick, 600 nm-wide.
- under external field, three DW velocity regimes: high mobility, low mobility and transition between them with negative differential mobility.
- the transition field between both mobilities is called Walker field, H_w (or Walker breakdown).
  $\rightarrow$ Below H_w: uniform DW movement
  $\rightarrow$ Above H_w: turbulent DW motion
  $\rightarrow$ similar to linear and turbulent motion in air.

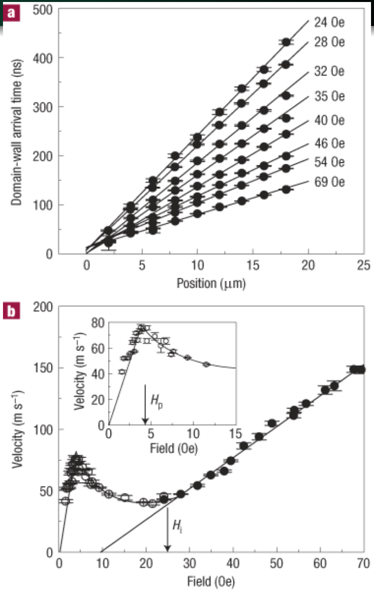

G.S.D. Beach et al, Nature Materials 4, 741 (2005)

Pushing domain wall by spin current:

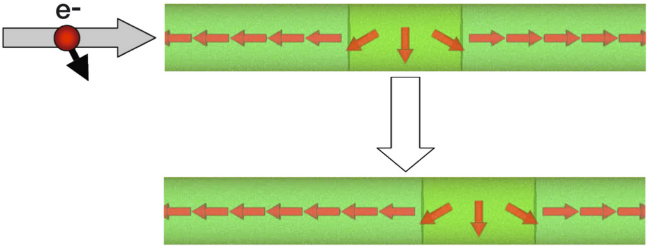

http://www.psi.ch/swissfe

LLG equation for magnetic domain:

$$\frac{d\bar{M}}{dt} = \gamma \bar{M} \times \bar{H} + \frac{\alpha}{M_s} \bar{M} \times \frac{d\bar{M}}{dt} - (\bar{u} \cdot \bar{\nabla}) \frac{\bar{M}}{M_s} + \beta \frac{\bar{M}}{M_s} \times [(\bar{u} \cdot \bar{\nabla}) \frac{\bar{M}}{M_s}]$$

last two terms describe the adiabatic and non-adiabatic spin-torque. The strength of the effect is given by u and the non-adiabaticity parameter β.

Domain wall speed when pushed by spin current

- Existence of critical current. Domain wall starts to move when this current is exceeded.
- oscillation of the domain wall between transverse wall and vortex wall has been observed.

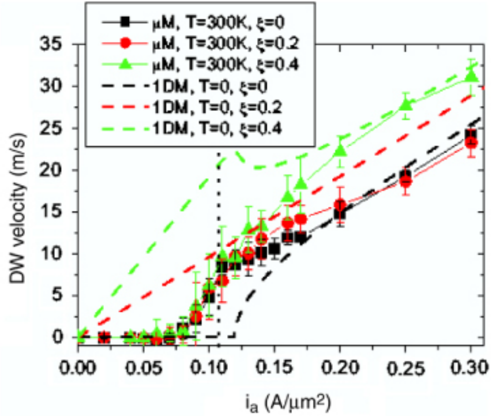

Martinez et al, J. Phys.: Condens. Matter 24, 024206 (2012)

Outline

Spintronics devices

- magnetic random access memory (MRAM)
- spin-transfer-driven microwave sources and oscillators
- read heads / hard disc drive
- race-track memory

Magentic random access memory (MRAM)

MRAM sketch

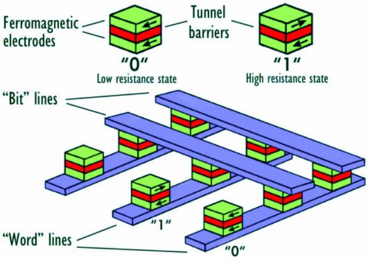

Bit state read by TMR effect.

First generation of MRAM: bit state written by magnetic field pulse.

Second generation MRAM: bit state written by spin-torque current.

Magentic random access memory (MRAM)

MRAM with writing by field pulse (first generation)

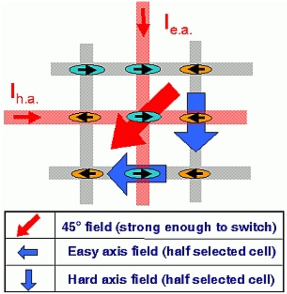

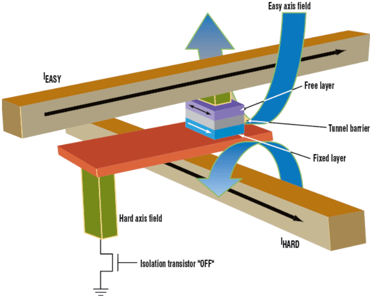

1. To write an MRAM bit, current is passed through a program line to generate a magnetic field. The sum of the magnetic field from both lines is needed to program the bit. To read an MRAM bit, current is passed through the bit and the resistance of the bit is sensed. (courtesy of Freescale)

Types of RAM memories:

Volatile RAM (need voltage to keep information) & non-voltaile RAM& ROM
Non-volatile RAM:

- EEPROM (Electrically Erasable Programmable Read-Only Memory), historically programmable ROM, later developed into flash memory. Based on metal MOSFET gate completely surrounded by isolator, and hence it can hold charge.

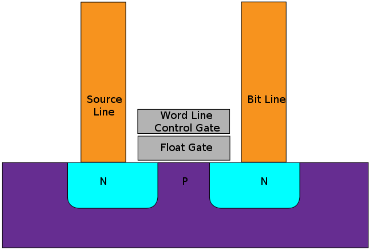

- SONOS (SONOS, short for "Silicon-Oxide-Nitride-Oxide-Silicon): improved EEPROM. Charge above the gate kept by Silicon Nitride Si_3N_4 with Ag nanoparticles.

Types of RAM memories:

Non-volatile RAM:

- MRAM
- PRAM (Phase-change memory). Similar to RRAM (Resistive random-access memory).
- FeRAM (Ferroelectric RAM (FeRAM, F-RAM or FRAM))
- Millipede: large array of AFM levers.

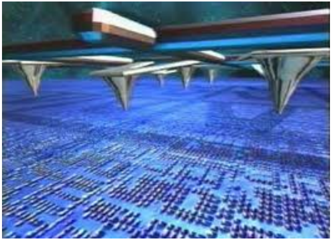

Hard-disk drive

Hard-drive mechanical principle:

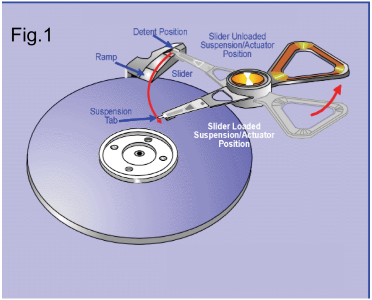

Picture of reading head:

Hard-disk drive (perpendicular recording)

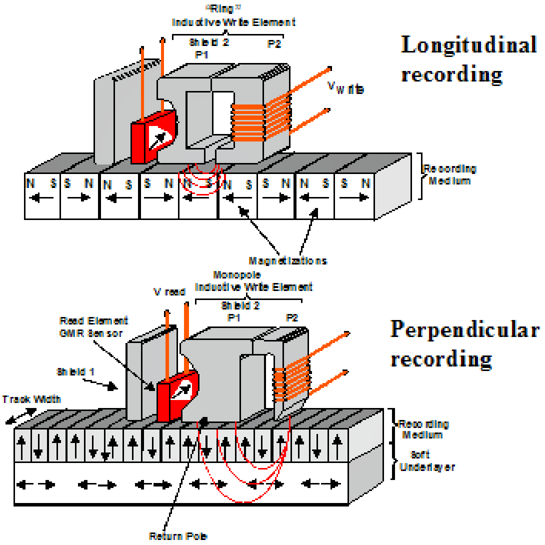

Physics of hard-drive

- plate: granular media, about 50 (?) grains per bit, nowdays perpendicular media used, todays capacity cca 1Tbit/in^2, i.e. ideal bit size about 25 nm. Perpendicular media required large uniaxial anisotropy: Pt/Co used, to overcome thermal stability problem. Dipolar and exchange mutual interaction between grains suppressed by using AFM coupling between grains. Also, plate must contain soft magnetic material to close magnetic circuit.
- head: writing & reading part, reading based on GMR or TMR, magnetic sensor. Writing still based on small magnetic coils. To reduce magnetic field strength needed for writing, thermal assisted writing is implemented.
- accurator (positioning head over the plate): Now, two stages accurator is used.

Race track memory

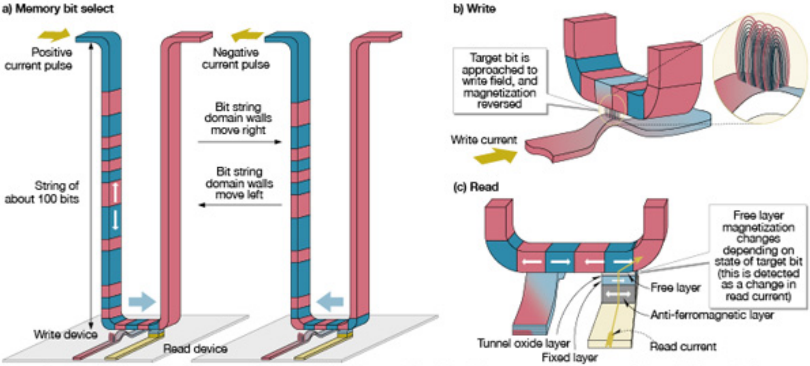

Using Current Pulses to Move Magnetic Domain Walls Magnetic Race-Track Memory records a string of about 100 bits of information perpendicularly to the Si substrate for each read/write device. This means information density is about 100 times higher than MRAM. Operating principles are shown for access memory bit select (a), write (b) and read (c). When selecting the memory bit for access a current pulse is applied to the magnetic material, causing the magnetic domain wall to move. A positive current pulse will move the wall to the right in the diagram, and a negative one to the left. The quantity of pulses can be controlled for random access, with data read executed after the target bit has been accessed. (Diagram by *Nikkei Electronics* based on material courtesy IBM)

Original idea of perpendicular race track memory is dead, but lateral race track memory still possible.

Outline

Hall effect

$$V_H = R_H \frac{IB}{d}$$

V_H: Hall voltage
R_H: Hall coefficient
d: plane thickness
B: magnetic field
I: current

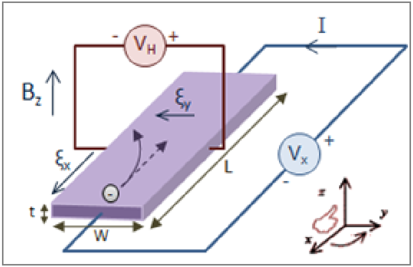

For simple metals:

$$R_H = -\frac{1}{ed}$$

n: charge carrier density
e: electron charge

In another expression:

$$\vec{E}_H = R_H \vec{j} \times \vec{B}$$

$\vec{E}_H$: induced electric field created by Hall effect
$\vec{j}$: current density

Spin-Hall effect / inverse Spin Hall effect

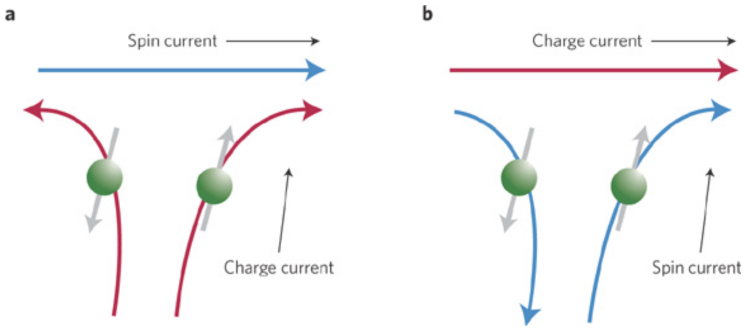

left: spin-Hall effect (conversion from charge current to spin current)
right: inverse spin-Hall effect (conversion from spin-current to charge current)

Spin-Hall effect / inverse Spin Hall effect

Can be explained as a scattering on impurity/defect or due to scattering caused by spin-orbit coupling [explain for charged impurity]

In vectorial form, spin-Hall effect is:

$$\vec{j}_{ch} =\sim [\hat{\sigma} \times \vec{j}_{sp}]$$
$$\vec{j}_{sp} = \alpha[\hat{\sigma} \times \vec{j}_{ch}]$$

- $\vec{j}_{ch}$: charge current
- $\vec{j}_{sp}$: spin current (vector determines current flow, not spin orientation)
- $\vec{\sigma}$: spin direction

Spin-Hall effect

Spin Hall effect:

- intrinsic: by spin-orbit coupling
- extrinsic: by charge impurities

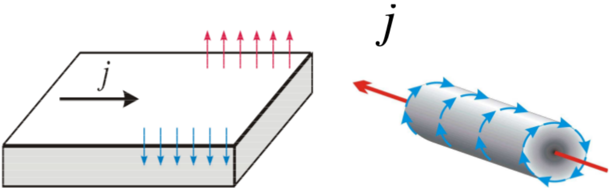

Figure 1. The Spin Hall Effect. An electrical current induces spin accumulation at the lateral boundaries of the sample. In a cylindrical wire the spins wind around the surface, like the lines of the magnetic field produced by the current. However the value of the spin polarization is much greater than the (usually negligible) equilibrium spin polarization in this magnetic field.

Non-local spin-Hall effect

(a) inverse spin Hall effect, conversion from the spin current to the charge current
(b) direct spin Hall effect, reversed conversion process from charge current to spin current.

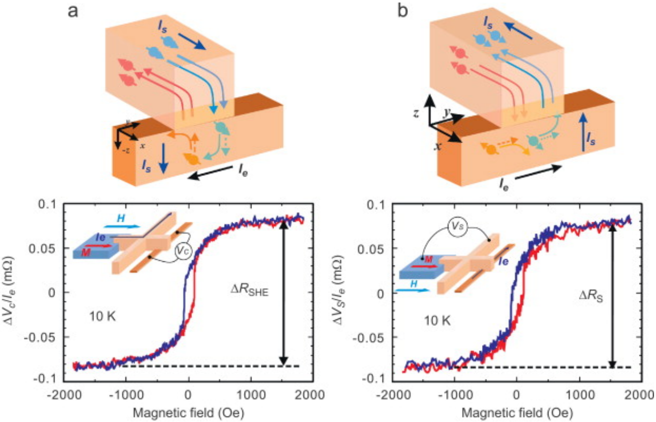

Y. Otani, Physica E 43, 735 (2011)

Spin caloritronics

Spin caloritronics addresses charge and heat flow in spin-polarized materials induced by temperature gradient.

No spin effect included:

In diffusive bulk metal (no spin effect included) (GEW Bauer, arXiv:1107.4395 (2011))

$$\begin{pmatrix} \mathbf{J} \\ \dot{\mathbf{Q}} \end{pmatrix} = \sigma \begin{pmatrix} 1 & S \\ \Pi & \kappa/\sigma \end{pmatrix} \begin{pmatrix} \boldsymbol{\nabla}_{\mathbf{r}} V \\ -\boldsymbol{\nabla}_{\mathbf{r}} T \end{pmatrix}$$

Gradient of potential (∇V) and gradient of temperature (∇T) cause flow of charge current (J) and flow of heat ($\dot{Q}$) [Onsager relations]

σ: electrical conductivity

κ: heat conductivity

S: Seebeck coefficient

$\Pi = ST$: Peltier coefficient

Spin caloritronics

When including also spin dependent transport (GEW Bauer, arXiv:1107.4395 (2011))

$$\begin{pmatrix} \mathbf{J}_c \\ \mathbf{J}_s \\ \dot{\mathbf{Q}} \end{pmatrix} = \sigma \begin{pmatrix} 1 & P & S \\ P & 1 & P'S \\ ST & P'ST & \mathcal{L}_0 T \end{pmatrix} \begin{pmatrix} \boldsymbol{\nabla}_{\mathbf{r}} \tilde{\mu}_c / e \\ \boldsymbol{\nabla}_{\mathbf{r}} \mu_s / 2e \\ -\boldsymbol{\nabla}_{\mathbf{r}} T \end{pmatrix}$$

Gradient of electrochemical potential ($\nabla\mu_c$), gradient of spin accumulation ($\nabla\mu_s$) and gradient of temperature (∇T) cause flow of charge current (J), flow of spin current (J_s) and flow of heat ($\dot{Q}$).

σ: electrical conductivity

P: spin polarization of the conductivity

P': derivative of P.

Spin Seebeck effect

Spin Seebeck effect: generation of the spin current by temperature gradient

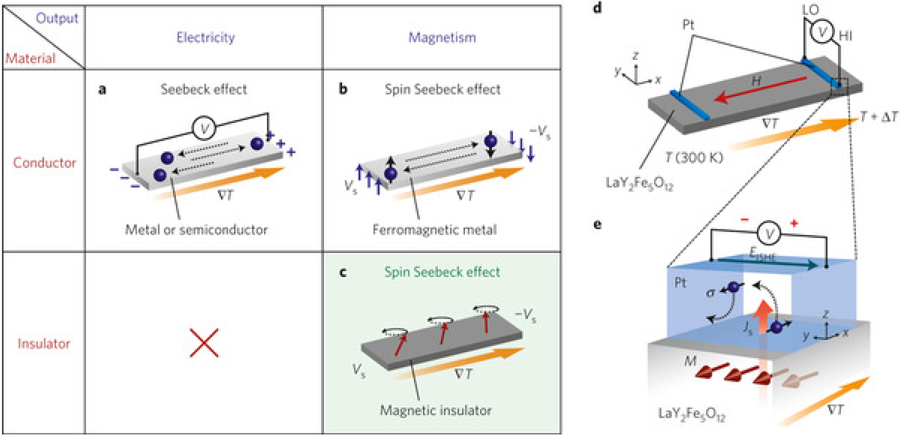

K. Uchida et al, Nat. Mat. 9, 894 (2010)

Configurations to measure spin-Seebeck effect

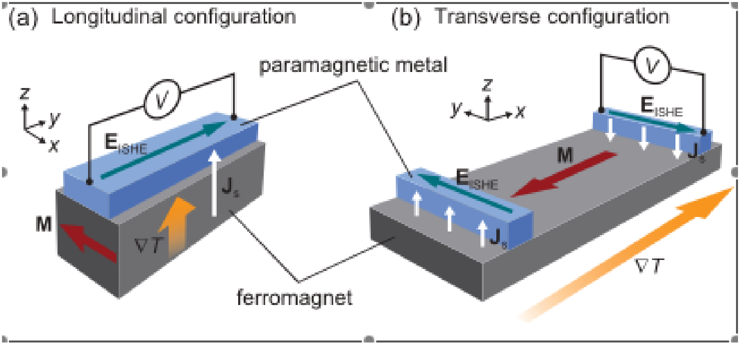

Uchida et al, arXiv:1111.3036 (2011)

- gradient of temperature creates spin current
- presence of spin current is detected by inverse spin-Hall effect (in paramagnetic metal).

Outline

Materials for spintronics

- ferromagnetic spin injectors/detectors: permalloy, Co, half-metals (Co_2FeSi, Co_2MnSi)
- spin conductors: Cu, Al, semiconductors. Now large development in organic spin conductors (small SO coupling $\Rightarrow$ small relaxation). Excellent results for spin-transport in graphene (2D carbon).
- spin absorbers: Pt, Au, Ag
- materials providing large spin-Hall effect (e.g. Au doped by 3% of Fe)
- material for tunnelling barrier: MgO, AlOx
- magnetic semiconductors (large effort, but currently mostly studied are diluted magnetic semiconductor (DMS), such as GaMnAs, but T_c only reached to to about 170 K; Mn content about 3-5%).

Specially developed materials for spintronics: DMS, half-metals.

Outline

Spins in semiconductors

Two branches of semiconductor spintronics

- semiconductor works as spin-conductor, the spin population is created by another way (using polarized light or using FM electrodes)
- semiconductor is ferromagnet (difficult to reach, working only for low temperatures now).

Properties of semiconductors as spin-conductor (compared to metals)

- long lifetime
- large spin-diffusion length
- small conductivity
- conduction also by holes
- electrons are well above Fermi level (hot electrons)

Spin injection to semiconductors

- optical spin orientation
- FM electrode through Schottky barrier
- FM electrode through TMR junction (MgO barrier)
- spin pumping
- using Rashba effect

Spin injection: through Schottky barrier

- spin injection through FM/semiconductor has poor spin injection due to conductance mismatch.
- creation of spin current:
  - spin injection through Schottky barrier.
  - spin injection through MgO tunnel burrier

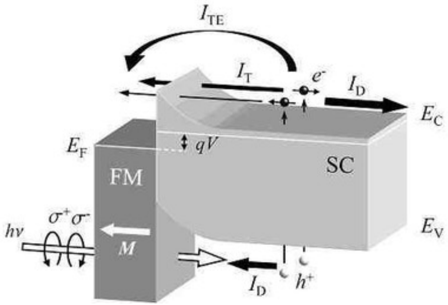

Optical spin orientation

- For $\hbar\omega$ between E_g and $E_g + \Delta_{SO}$, only the light and heavy hole subband contribute. Then for zinc-bland structure, the spin-polarization is $P_n = -1/2$.
- Light polarization can also be used to detect spin polarization in semiconductors.

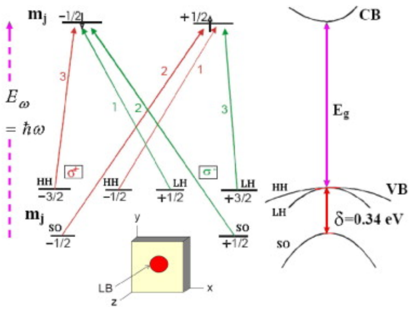

Rashba effect I

Rashba Hamiltonian:

$$H_R = \alpha(\sigma \times \vec{p}) \cdot \hat{z}$$

α: Rasba coupling
$\vec{p}$: electron's momentum
σ: spin direction (Pauli matrix vector)

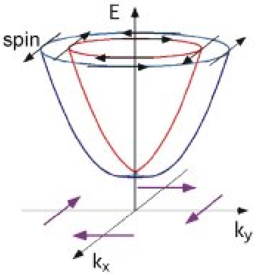

The Rashba effect is a momentum dependent splitting of spin bands in two-dimensional condensed matter systems (heterostructures and surface states). It originates from concurrent appearance of

- spin-orbit coupling
- asymmetry of the potential in the direction perpendicular to the two-dimensional plane

Rashba effect II

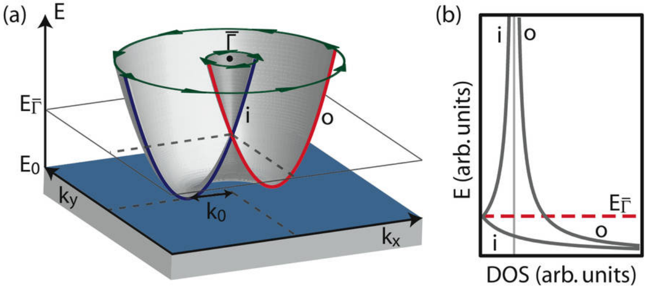

http://www.sps.ch/fr/articles/progresses/

- For $\vec{p} = p_x$ and $H_R = \alpha(\tilde{\sigma} \times \vec{p}) \cdot \hat{z} \Rightarrow H_R = -\alpha p_x \sigma_y$
- splitting of energy states according to $\vec{p}$ and $\vec{\sigma}$ directions.
- max. splitting when z, $\vec{p}$ and $\vec{\sigma}$ are perpendicular each other.
- inversion symmetry must be broken (i.e. for centrosymmetric crystal Rashba originates from interface. In that case, can be enhanced/suppressed by an external electrical field $\Rightarrow$ *control of spin by an external electrical field*).

Hanle effect

Hanle effect:

- dependence of the spin accumulation on magnetic field applied perpendicular to the injected spin
- spins are under magnetic field ⇒ spin precession
- due to diffusive movement of electrons, they move forward at different speeds ⇒ dephasing appears, reducing average spin accumulation

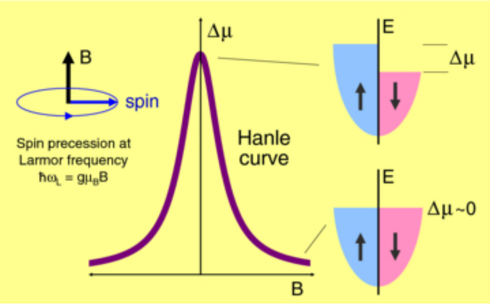

http://iopscience.iop.org/0268-1242/27/8/083001/

Example of Ge structure with measured Hanle effect

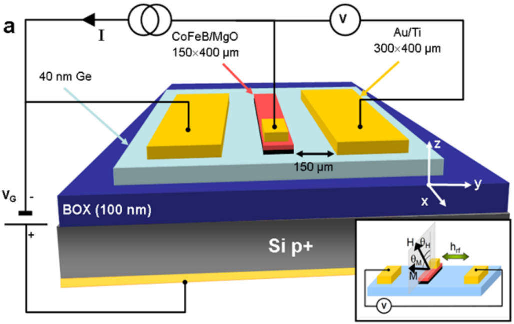

Inverse spin-Hall effect (ISHE)
(spin current generatd by FMR, transported in Ge, converted to I_{ch} by ISHE)

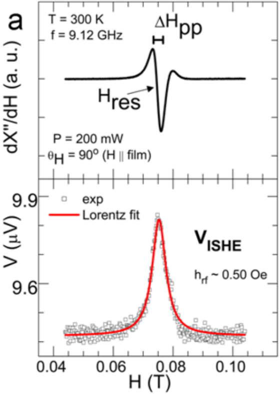

Hanle and inverse Hanle effect:

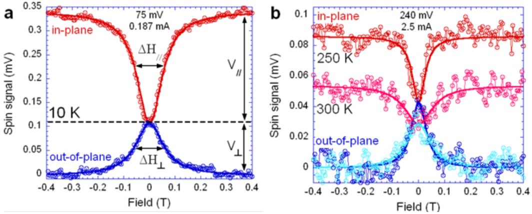

Jain et al, PRL109, 106603 (2012); `http://arxiv.org/pdf/1203.6491v2.pdf`